공학박사 학위논문

Conductive Foam-surfaced Electrode for Capacitively-coupled EEG Measurement in Brain-Computer Interface

뇌-컴퓨터 인터페이스에서 용량성 결합 뇌파 측정을 위한 전도성 폼 표면 전극

2013년 02월

서울대학교 대학원

협동과정 바이오엔지니어링 전공

백 현 재

Conductive Foam-surfaced Electrode for Capacitively-coupled EEG Measurement in Brain-Computer Interface

뇌-컴퓨터 인터페이스에서 용량성 결합 뇌파 측정을 위한 전도성 폼 표면 전극

지도교수 박 광 석

이 논문을 공학박사 학위논문으로 제출함
2013년 02월

서울대학교 대학원
협동과정 바이오엔지니어링 전공
백 현 재

백현재의 공학박사 학위논문을 인준함
2013년 02월

위 원 장 김 희 찬_____ (인)

부위원장 박 광 석_____ (인)

위 원 성 정 준_____ (인)

위 원 이 태 수_____ (인)

위 원 임 용 규_____ (인)

Ph. D. Dissertation

Conductive Foam-surfaced Electrode for Capacitively-coupled EEG Measurement in Brain-Computer Interface

Hyun Jae Baek

February, 2013

Interdisciplinary Program in Bioengineering
Seoul National University

Conductive Foam-surfaced Electrode for Capacitively-coupled EEG Measurement in Brain-Computer Interface

By

Hyun Jae Baek

Interdisciplinary Program in Bioengineering,

Seoul National Univerisity

This dissertation is approved for

The Degree of Doctor of Philosophy

February, 2013

Chairman _____

Kim, Hee Chan, Ph.D.

Vice Chairman _____

Park, Kwang Suk, Ph.D.

Member _____

Sung, Jung Joon, M.D., Ph.D.

Member _____

Lee, Tae Soo, Ph.D.

Member _____

Lim, Yong Gyu, Ph.D.

Abstract

Conductive Foam-surfaced Electrode for Capacitively-coupled EEG Measurement in Brain-Computer Interface

Hyun Jae Baek

Interdisciplinary Program in Bioengineering

The Graduate School

Seoul National University

Brain-computer interface (BCI) technologies have been intensively studied as a means to provide alternative communication tools that are entirely independent of neuromuscular activities. Current BCI technologies use electroencephalogram (EEG) acquisition methods that require unpleasant gel injections, impractical preparations, and clean-up procedures. The next generation of BCI technologies requires practical, user-friendly, nonintrusive EEG platforms that will facilitate the application of laboratory work in real-world settings. A capacitively-coupled electrode that does not require electrolytic gel or direct electrode-scalp contact is a potential alternative to the conventional wet electrode in future BCI systems.

In this paper, a new conductive polymer foam surfaced electrode was proposed for use as a capacitively-coupled EEG electrode for nonintrusive EEG measurements in out-of-hospital environments. The current capacitively-coupled electrode has a rigid surface that produces an undefined contact area due to its stiffness, which renders it unable to conform to head curvature and locally isolates hairs between the electrode surface and scalp skin, thereby complicating EEG measurement through hair. This issue was overcome by applying a conductive polymer foam to the high-input-impedance active electrode surface to provide a cushioning effect. This enabled EEG measurement through hair without any requirement for conductive contact with bare scalp skin. Experimental results showed that the new electrode provided lower electrode–skin impedance and higher voltage gains, signal to-noise ratios, signal-to-error ratios, and correlation coefficients between EEGs measured by capacitively-coupled and standard resistively-coupled methods when compared to a conventional capacitively-coupled electrode. In addition, the new electrode could measure EEG signals, while the conventional capacitively-coupled electrode could not. The expectation is that the new electrode presented here can be easily installed in a hat or helmet to create a nonintrusive wearable EEG apparatus that does not make users look strange for real-world EEG applications.

This paper also presents results from five subjects who exhibited visual or auditory steady-state responses according to BCI using these new capacitively-coupled electrodes. The steady-state visual evoked potential (SSVEP) spelling system and the auditory steady-state response (ASSR) binary decision system were employed. Offline tests demonstrated classification accuracies high enough to be used in a BCI system (95.2% for SSVEP BCI (6s), 82.6% for ASSR BCI (14s)) with analysis time slightly longer than that reported in the literature when wet electrodes were employed with the same BCI system. Subjects performed online BCI under the SSVEP paradigm in copy spelling mode and under the ASSR paradigm in selective attention mode with a mean information transfer rate (ITR) of 17.78±2.08 and 0.7±0.24 bpm, respectively. The results of these experiments demonstrate the feasibility of using the proposed capacitively-coupled EEG electrode in BCI systems. This electrode may become a flexible and non-intrusive tool fit for various applications in the next generation of BCI technologies.

Keywords: biomedical electrode, brain-computer interface (BCI), capacitive sensors, electroencephalography, polymer foams.

Student Number: 2009-30267

Contents

List of Tables

List of Figures

List of Abbreviations

ABCI	Augmented Brain-Computer Interface
ACC	Accuracy
ASSR	Auditory Steady-State Response
BCI	Brain-Computer Interface
CCA	Canonical Correlation Analysis
DRL	Driven-Right-Leg
EEG	Electroencephalogram
EFF	Efficiency
ITR	Information Transfer Rate
LDA	Linear Discriminant Analysis
LPM	Letters per Minute
NUM	Number of Correct Decision
SEM	Scanning Electron Microscope
SENS	Sensitivity
SER	Signal-to-Error Ratio
SNR	Signal-to-Noise Ratio
SPEC	Specificity
SSVEP	Steady-State Visual Evoked Potential
QoLT	Quality of Life Technology

1. Introduction

Recent advances in biomedical engineering during the past several decades have led to improvements in quality of life technologies (QoLT) including patient care, personal/ubiquitous healthcare and assistive technology for disabled people [1-5]. Biological signal monitoring plays a critical role in QoLT since many of these technologies use biomedical signals as input [6-9]. Therefore, the development of innovative biomedical electrode is one of the most significant factors in the realization of these types of QoLTs. The setting for QoLTs should not be limited to clinical laboratory environments, but may be any location, such as in the home or the workplace, where personal care and support for daily living are provided. Therefore, the recording of biomedical signals by electrocardiography (ECG), electromyography (EMG) and electroencephalography (EEG) should be simple, ambulatory and convenient. The conventional silver/silver chloride (Ag/AgCl) electrode used in current clinical laboratory procedures produces real charge current contact between the electrode and the body. It does so by employing an electrolytic gel that reduces the electrode-skin interface impedance by making its dry layer ion conductive. Although these wet electrodes are universally accepted, they still have limitations for out-of-hospital measurements.

1.1. The Brain-Computer Interface

The brain-computer interface (BCI) is an emerging technology useful for interacting with external world through a non-muscular communication channel, completely independent of the motor pathways of the neural system [10]. The traditional goal of a BCI system is to provide helpful communication tools for improving the quality of life of disabled users who cannot move freely because of neural disease such as amyotrophic lateral sclerosis (ALS), brainstem stroke, or spinal cord injury [11, 12]. Rapid progress is being made to reach these goals set by most BCI research groups. However, recent BCI research has expanded the traditional role of BCI from communication to rehabilitation through neuro-feedback for stroke, autism, attention deficit hyperactivity disorder (ADHD), and other disorders [13, 14]. Now, not only patients with severe disabilities, but also people with less severe disorders or even healthy individuals, are potential candidates for BCI technologies (figure1-1). Therefore, today's BCI research should consider applications of BCI technologies that extend beyond the hospital or laboratory environments. BCI should be available for use by any individual at any time and in any place.

Typically, a BCI system comprises three major components as shown in figure 1-2 [15]. The first part is the brain signal acquisition unit which acquires signals from the brain by electrodes placed on the user's scalp or cortical surface; similarly, signals

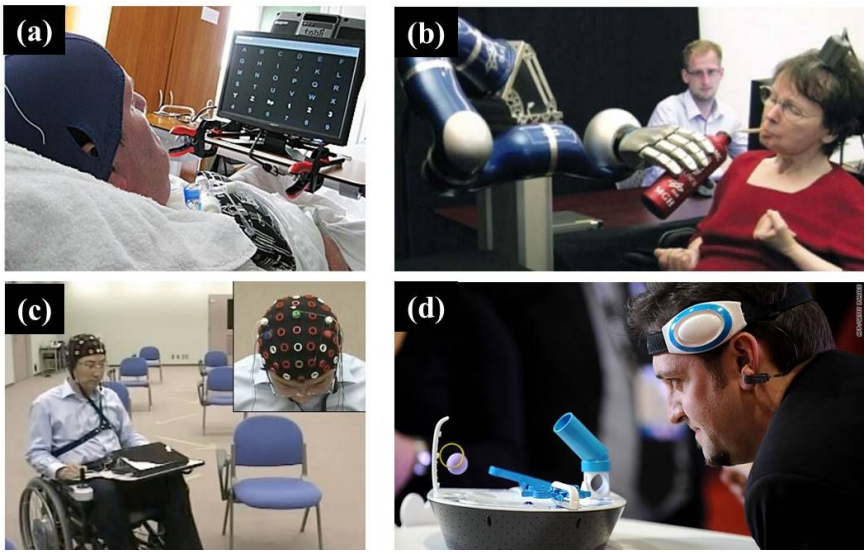

Figure 1-1. Examples of BCI systems: (a) EEG-based P300 mental speller, (b) ECoG-based robotic arm control, (c) EEG-based wheelchair control and (d) BCI entertainment.

within the brain may be obtained by one of a number of techniques including near infrared spectroscopy (NIRS), electrocorticography (ECoG), or electroencephalography (EEG). The second part of the system is the signal processing unit, which processes signals from the brain to extract specific signal features that reflect the user's intent, and can subsequently be used as commands or messages that operate devices. The last part is the application unit, which uses the processed signals to drive an application. This application can be a virtual keyboard or devices external to the user, such as a prosthetic arm or other equipment.

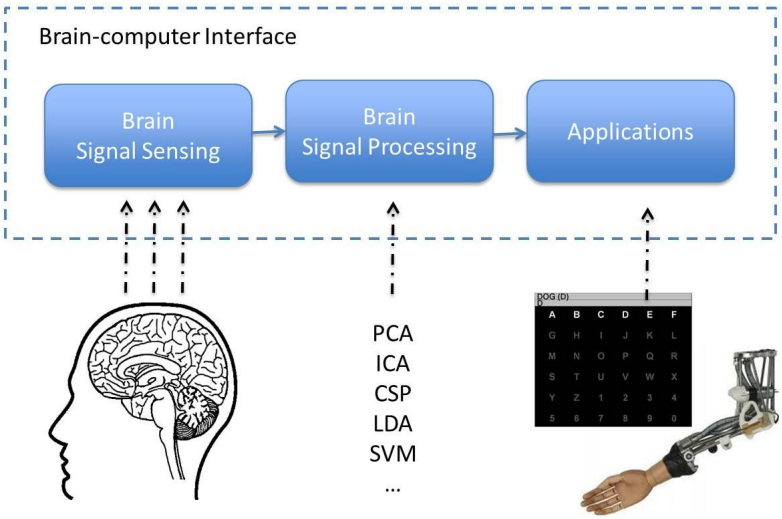

Figure 1-2. Components of a brain-computer interface (BCI): (1) brain signal sensing part, (2) brain signal processing part and (3) Application part.

BCI has been growing rapidly over the past 20 years and various systems have been introduced. Most BCI research has focused on signal processing and application units in order to enhance BCI system performance with respect to accuracy, information transfer rate (ITR) or the number of possible selections [16, 17]. Experimentation has not delved into new or innovative brain signal sensing technologies because current clinical modalities have provided excellent quality signals. However, in order to produce a BCI system that is practical for today's wide range of potential users, the brain signal acquisition method should be carefully considered as well.

1.2. EEG Electrodes

The electroencephalogram (EEG) is a noninvasive recording of the brain's spontaneous electrical activity obtained at the scalp surface. EEG is valuable tool for clinical diagnosis of epilepsy, encephalopathies and brain death as well as in research areas including psychophysiology, cognitive science and neural engineering [18-20].

The current flow in the human body is due to ion flow, not electrons. Activation of neurons produces local ionic current flows. The brain electrical current consists mostly of Na^{+}, K^{+}, Ca^{++}, and Cl^{-} ions that are pumped through channels in the neurons and membranes in directions governed by membrane potential. The EEG electrodes sense the current from the neuronal layers after it penetrates through the skin, skull and several other layers [21]. The electrodes form an electrical transducer to convert ionic current flow in the scalp into electron flow that can be detected by an electronic amplifier. Currently, a remarkable variety of different types of electrodes have been introduced for recording potentials on the body surface including EEG. The present section describes the classification of electrodes types and gives examples of each.

1.2.1. Polarizable /Nonpolarizable Electrode

A biopotential electrode is a transducer that senses the ion distribution on the surface of tissue, and converts that ion current to an electron current. An electrolyte solution is placed on the side of the electrode that comes into contact with tissue; the other side of the electrode consists of conductive metal attached to a lead wire connected to the instrument. A chemical reaction then occurs at the interface between the electrolyte and the electrode. The metal electrode discharge ions into solution when it comes in contact with an electrolyte; some of these discharged ions may be tightly bound to the surface of the electrode. Concomitantly, an adjacent layer of oppositely charged ions from the solution is formed, resulting in the creation of the so called electrical double layer at the metal-electrolyte interface. The difference in the rate of these two processes results in a voltage appearing at the electrode and this is termed the half cell potential. If there is a current, the observed half cell potential is altered due to polarization of electrode. Polarizable (nonreversible) electrodes are those in which no actual charge crosses the electrode-electrolyte interface when a current is applied. Polarizable electrodes act more like a capacitor and current is displaced but does not move freely across the electrolytic interface. Metal electrodes come closest to behaving like polarizable electrodes since the materials are relatively

inert; they are difficult to oxidize and dissolve. Instead, changes in the concentration of ions occur at the interface. On the other hand, nonpolarizable (reversible) electrodes are those in which current passes freely across the electrode-electrolyte interface, with no requirement for energy to make the transition.

1.2.2. Dry /Wet Electrode

Wet electrodes use a gel (or paste) type electrolyte between the electrode and the surface of skin. The most common type of wet electrode is the pre-gelled Ag/AgCl electrode. Its characteristics approach those of a perfectly nonpolarizable electrode. The electrode metal is made up of Ag, which is coated with an AgCl layer. An electrolyte gel is used to estabilish the electrical contact between the electrode and the surface of the skin. Wet electrodes can also be polarizable electrodes; for example, disk cup electrodes which are made of gold, platinum, or stainless steel are polarizable electrodes. However, they are classified as wet electrodes since they are used with conduction paste. The most important advantages of the wet electrodes are their low impedance and low artifact due to the motion. On the other hand, the use of gel/paste creates discomfort and increases the preparation time for using the acquisition system. Dry electrodes, as their name implies, do not use any kind of gel

or paste to make contact between the electrode and the skin. Therefore, they are more comfortable and easier to prepare for use compared to the wet electrodes. However, due to the lack of the electrolyte, their characteristics are closer to polarizable electrodes, which can be characterized as a leaky capacitor, resulting in relatively higher contact impedance and motion artifacts.

1.2.3. Capacitively-coupled / Resistively-coupled Electrode

The electrodes can be either resistively-coupled or capacitively-coupled to the skin. Theoretically, nonpolarizable electrodes, for which a faradic current can freely pass without polarization act like resistors, while polarizable electrodes, which are characterized by an absence of net current between the two sides of the electrical double layer, act like capacitors. Therefore, all kinds of polarizable electrodes, such as dry metal electrodes, can be classified as capacitively-coupled electrodes. However, in practice, a metallic surface in direct contact with the bare skin uses a parallel combination of resistive and capacitive coupling to the local skin potential and they are not named capacitively-coupled electrode. Capacitively-coupled electrode do not directly contact bare skin; the electrode-skin interface is replaced by external insulation layers such as cloth, hair, or dielectric film. The recording surface

is insulated by a dielectric substance and the skin electrode junction behaves as a pure capacitor. There is no electrical contact between the electrode and skin; therefore, these are often called non-contact or insulated electrodes. In this case, designing active electrodes with ultrahigh input impedance is essential because of the very small coupling capacitance.

1.2.4. Other Classifications

Electrodes can be classified as reusable or disposable. Disposable electrodes are utilized only for a single patient and then discarded. The disposable electrodes have largely resulted from attempts to reduce the costs involved in the upkeep and cleaning of the electrodes between users and to reduce electrode preparation time required prior to each use of the electrodes. Most of the disposable electrodes retain metallic (silver/silver chloride) portions embedded within a packaged conductive electrolyte gel (pre-gelled electrode). On the other hand, reusable electrodes have unlimited shelf life, as their name suggests. They are usually metallic, made of silver or nickel silver, and are cleaned between uses with an antiseptic agent such as alcochol. Most of dry electrodes are reusable and some of them even do not require a cleanup procedure between uses.

Electrodes can be classified as surface-, internal- or micro electrodes according to their applications. Surface electrodes are placed in contact with the skin and are most widely employed for recording potentials on the body surface. Metal plate electrodes, suction electrodes, and floating electrodes belong to the surface electrode category. Electrodes also can be used within the body to detect biopotentials; these are called internal- or percutaneous electrodes. These electrodes differ from surface electrodes in that they do not have to contend with the electrolyte-skin interface and its associated limitations. Representative examples are needle and wire electrodes. Microelectrodes are often used to measure biopotentials at the cellular level. In order to measure intracellular potential, the electrode should be small (approximately 0.05 to 10μm) and strong so that it can penetrate the cell membrane and remain mechanically stable.

Finally, electrodes can be classified as active or passive. Typical electrodes are passive electrodes that require only one wire per electrode for signal transmission while active electrodes require multiple wires per electrode for a power supply. The active electrodes are electrodes with very low output impedance and contain electronic circuitry at the electrode end. The active electrode is a superior solution for the problem of interference pickup of the cables, and provides the best possible suppression of interference by impedance transformation directly on the electrode.

1.2.5. Direct Comparison of Electrodes

This section describes a brief comparison of six kinds of bioelectrodes based on tests involving impedance and electrocardiogram waveform analysis. Data were collected at the same measurement locations in the same physical environment for all electrodes. Testing electrodes were: 1) a pre-gelled Ag/AgCl electrode (3M Red Dot foam monitoring electrode 2225, 3M Health Care, St.Paul, MN); 2) a dry Ag/AgCl limb clamp electrode (EL-001, Gmedi Co., Ltd., Seoul, Korea); 3) a conductive fabric electrode (Silver Fabric, A-Jin Electron, Busan, Korea); 4) a stainless steel limb clamp electrode (Clip-RE/Clip-YE, Laxtha Inc., Daejeon, Korea); 5) a disk cup electrode (Gold-disk cup electrode, Grass Technology, West Warwick, RI, USA); and 6) a laboratory-made capacitively-coupled electrode. The transfer function is the quotient of the cross power spectral density (P_{21}) of ECGs measured using a pre-gelled Ag/AgCl electrode (Sig_1) and one of the other electrodes (Sig_2) and the power spectral density (P_{11}) of ECGs measured using a pre-gelled Ag/AgCl electrode, $T_{21}(f)= P_{21}(f)/ P_{11}(f)$. The transfer function has a magnitude and a phase as indicated in figure 1-3. It has been estimated by averaging the single ECG waveforms illustrated in figure 1-4. Comparison disclosed a relatively flat transfer function magnitude and no phase delay for skin-contact electrodes, while a clear high pass

effect was found for the capacitively-coupled electrode. Averaged ECG waveforms showed no significant differences except for the ECG measured using the capacitively-coupled electrode. Continuous ECG signals illustrated in figure 1-5 also showed differences in background noise level. Differences in impedance in relation to the frequency range of 0.1Hz-1kHz were also noted, as shown in figure 1-6. Note that the reason for the significantly higher impedance of the gold disk-cup electrode might be the small electrode size.

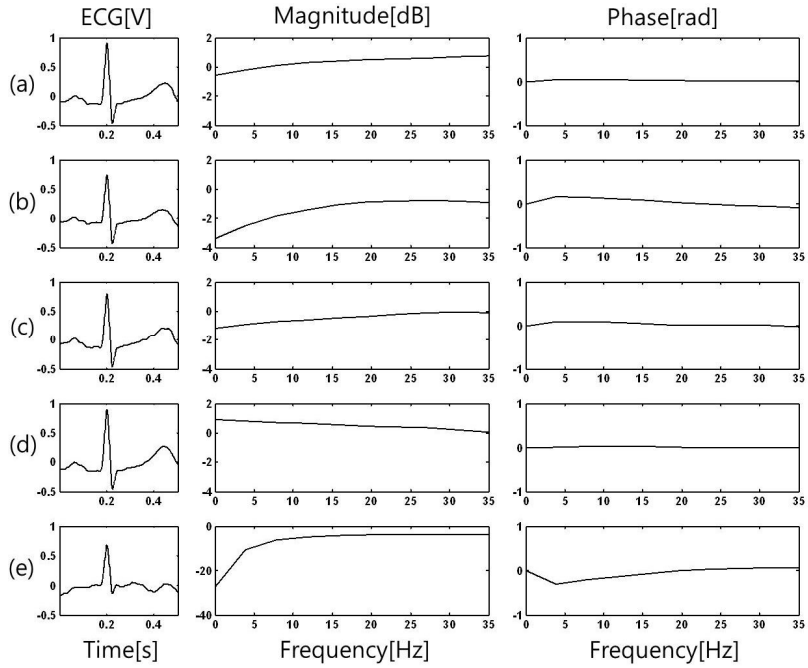

Figure 1-3. Transfer function of the averaged ECG waveform: (a) dry Ag/AgCl, (b) Textile, (c) Disk-cup, (d) Stainless Steel and (e) Capacitively-coupled

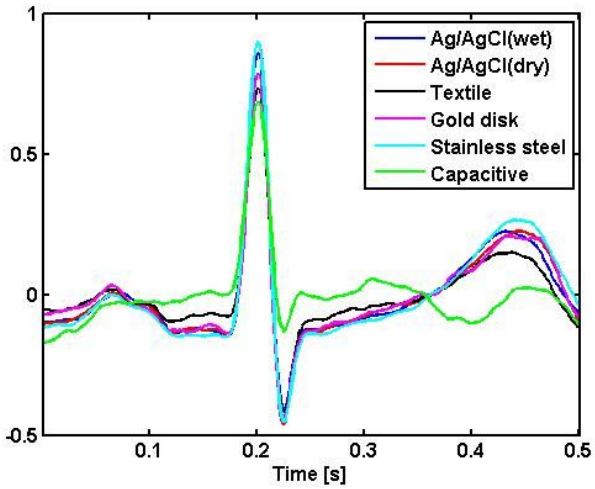

Figure 1-4. ECG waveforms averaged based on a QRS complex.

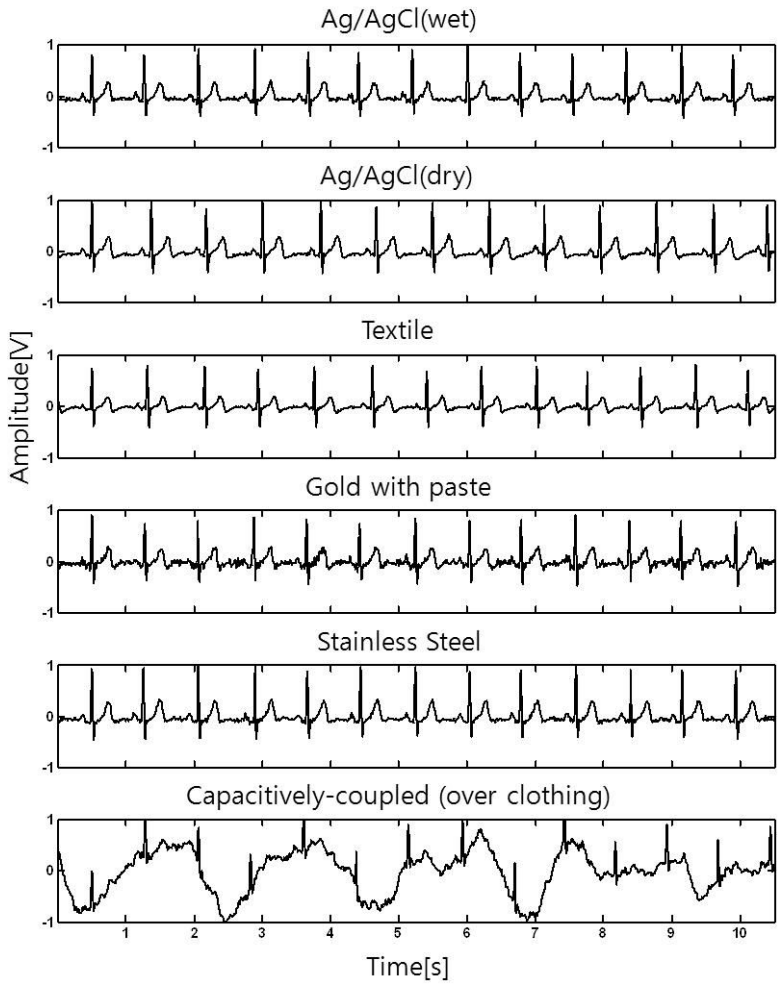

Figure 1-5. ECG signals from the pre-gelled Ag/AgCl electrode, dry Ag/AgCl electrode, textile electrode, disk-cup electrode, stainless steel electrode and capacitively-coupled electrode.

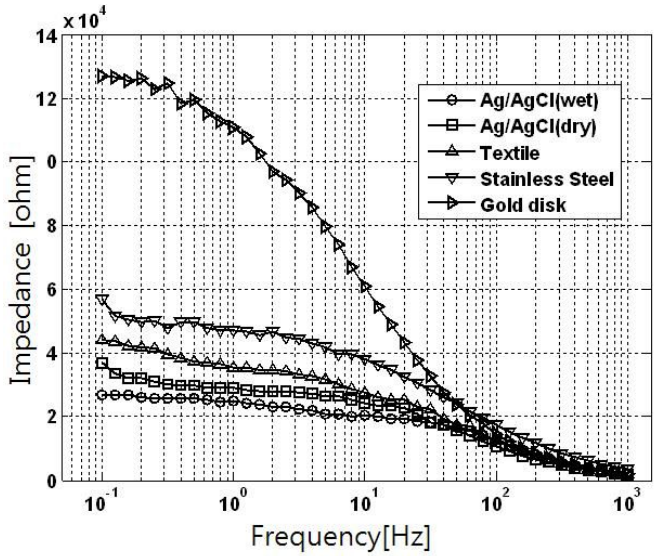

Figure 1-6. Impedances according to the frequency changes (0.1Hz-1kHz).

The work described here demonstrated that skin-contact type electrodes influence general noise characteristics rather than specific waveform distortion, when compared to a non skin contact type capacitively-coupled electrode. Comparison of biopotential recording electrodes expressed in other studies regarding static interference, motion artifact and offset potential was not supported by the work described here [22, 23]. Each electrode type has its own characteristics; its own pros and cons in relation to measurement conditions, application purpose, and the electronic specifications of the recording amplifier. Based on related literature and our investigations, we could conclude that a reasonable level of bio-potential signal can be acquired using these electrodes at least for non-medical purposes.

1.3. EEG Measurement in BCI

The EEG is the most commonly used method of signal acquisition for BCI because of its cost-effectiveness, portability, and noninvasiveness. Currently, EEG-based BCI systems require silver/silver chloride (Ag/AgCl) electrodes that employ real charge current contact between electrodes and scalp tissue. Ag/AgCl electrodes have been well studied and characterized for many decades. However, despite the historical and universal acceptance of classical Ag/AgCl electrodes, they are inconvenient for use in out-of-hospital applications such as brain computer interface (BCI). The setup procedure is time-consuming, expensive and intrusive for subjects. The use of Ag/AgCl electrodes requires scalp/hair preparation and conduction gel to reduce scalp-electrode interface impedance. Gel is wet and may dry out, thereby causing the impedance to vary, and may also cause short circuits between EEG electrodes in close proximity. In addition, hair must be washed after use and gel may leave residues on the scalp, possibly causing allergic reactions. Finally, electrode attachments including conventional EEG caps make subjects look unusual, making daily EEG monitoring inconvenient. For out-of-hospital EEG applications, dry electrodes that do not require adhesive paste or gel and more aesthetic EEG systems should be considered.

Significant advances have been made in dry electrode technologies for bio-potential

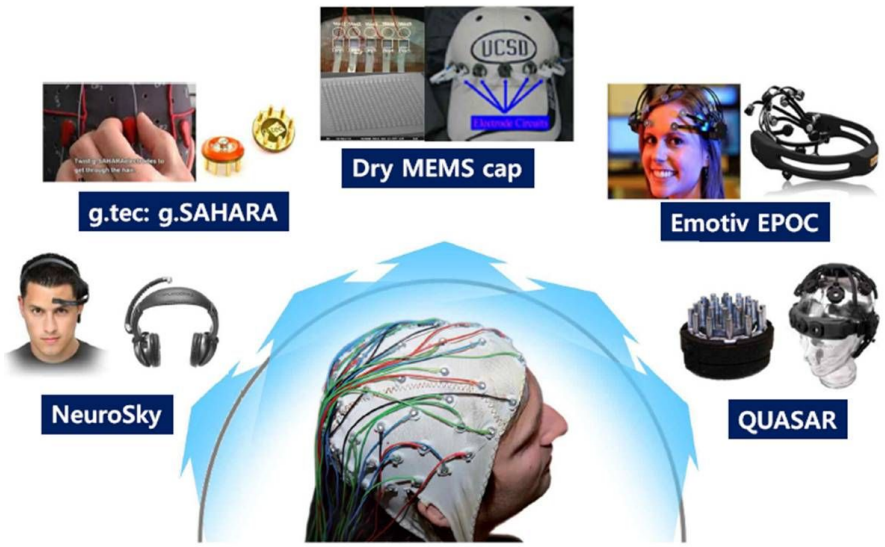

Figure 1-7. Dry EEG electrode system: Neurosky single channel headset, g.tec g.SAHARA electrode, dry MEMs cap, Emotive Epoc multi-channel headset, QUASAR hybrid electrode system (from left to right).

measurement, mostly focused on electrocardiograms (ECG) [24-26]. However, since the sites for EEG electrode placements are mostly covered with hair and the EEG is weaker than other bio-potential measurement tools, the use of dry electrodes can be difficult. Most dry EEG electrodes make signal measurements by penetrating the outermost layer of the skin—the stratum corneum—using microelectromechnical (MEMS) or carbon nanotube techniques [27-29]. However, these types of dry electrodes are still somewhat invasive, and the risk of infection by electrodes that penetrate tissue persists. In addition, the EEG cannot be recorded through hair and therefore hair and scalp preparation is required to make signal measurements.

Other needleless dry electrodes employ metal electrodes with no electrolyte [30-32]. These electrodes are fully noninvasive and do not require conductive gel or paste between the skin and electrode surfaces. However, they also require preparation to make contact between the scalp and electrode (figure 1-7). Dry EEG electrodes are possible solutions for nonclinical long-term signal recording with increased practicality, efficacy and ease of use. For practical use, they should avoid typical EEG preparation procedures, including head measurement, for accurate electrode placement according to the international 10-20 montage and scalp-hair preparation involving abrasive paste or gel. Finally, these electrodes should not make users uncomfortable or look unusual. It should be possible to make EEG signal measurements while simply wearing caps with EEG electrodes installed in appropriate montages. EEG signals should be recorded over the hair without the need to remove scalp hair.

1.4. Problem Statement

The solution for these requirements could be capacitively-coupled electrodes, which are already well documented in the literature [33, 34]. A capacitively-coupled electrode measures biopotentials such as ECG, EMG, and EEG despite insulation by cloth or hair; therefore, biopotentials can be easily and naturally recorded from

capacitively-coupled electrodes installed in items of daily use such as a bed, chair, or helmet without direct skin contact and without preparation procedures. However, unlike capacitively-coupled ECG monitoring, the application of capacitively-coupled electrodes for EEG measurement requires more considerations since the capacitively-coupled measurement of biosignals is heavily dependent on a coupling capacitance building up between the scalp surface and the electrode surface. Human hair is thin and creates an irregular surface between the electrode surface and the scalp. As a result, fine air gaps are formed between the scalp and electrodes. In addition, hair moves easily during measurements. Electrodes easily slip over hair, causing changes in impedance. Coupling capacitance is sensitive to these factors, which readily yield noise in the results. Finally, these problems make capacitively-coupled EEG measurement difficult and impractical. Figure 1-8 shows a simplified conceptual diagram of capacitively-coupled electrode application for EEG measurement. The rigid surface of a conventional capacitively-coupled electrode is unable to adapt to the head curvature. As an insulator, hair forms an irregular surface including hundreds of micrometer-wide air gaps between the scalp and the electrode surface. The head curvature and the irregular surface leads to the loss of contact area and results in increased contact impedance. The motion of the electrodes relative to the hair and head curvature creates artifacts in the measured signals.

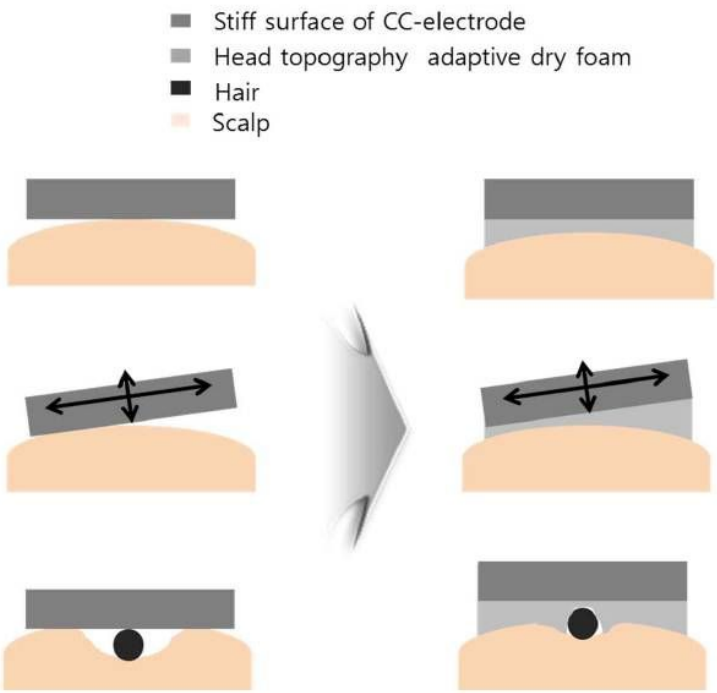

Figure 1-8. Conceptual conditions of capacitively-coupled electrode application for EEG measurement. (*top*) rigid surface of electrode is unable to adapt to the head curvature, (*middle*) motion of electrode relative to the hair and head curvature creates artifacts in EEG, (*bottom*) hair makes micrometer-wide air gaps between the scalp and the electrode leading to the loss of contact area and resulting in increased contact impedance.

1.5. Purpose of the Study

The present study was motivated by the following two functional aims: 1) enhancement of a capacitively-coupled electrode specifically focused on EEG measurement through hair and 2) its application for non-medical purposes such as a brain-computer interface (BCI). This paper describes a capacitively-coupled electrode whose surface is adaptive to head topography and its performance in EEG measurement through hair without direct conductive scalp contact.

The problems described in section 1.3 were overcome by investigating a capacitively-coupled electrode with a soft dry foam surface. The concept of this study was inspired by Gruetzmann et al. [35] and applied to a capacitively-coupled electrode. It adapts to scalp topography such as head curvatures and hair due to its cushioning effect, therefore providing a more effective contact area. In addition, the new electrode maintains stable contact under motion, reducing the sliding of the electrode over the hair due to its cushioning effect and textures. The study was approved by the Institutional Review Board of Seoul National University Hospital, Korea, and the participants provided written informed consent at the start of the experiments. The study about a conductive polymer foam surfaced capacitively-coupled electrode was published as a journal paper [36]. A study on brain-computer interface using capacitively measured EEGs is in revision by a journal [37].

2. Methods

A capacitively-coupled electrode measures an EEG through the capacitance, C_S, established between scalp surface and electrode over hair as shown in figure 2-1. It effectively relies on detecting the displacement current, I_D, which is proportional to the rate of change of the electric field associated with the source EEG signal, V_S. Voltage gain of the capacitively-coupled electrode can be expressed very simply as equation (2-1) if we consider source voltage, V_s, coupling capacitance C_s and gain of voltage follower is 1 ($V_{in} = V_{out}$).

$$G_S = \frac{V_{out}}{V_S} = \frac{j\omega R_{in} C_S}{1 + j\omega R_{in}(C_{in} + C_S)} \qquad (2\text{-}1)$$

Equation (2-1) shows that the capacitively-coupled measurement of the EEG requires a large coupling capacitance, C_S, and a very high input impedance of the electrode amplifier. Coupling capacitance should be much larger than input capacitance, C_{in}. Coupling capacitance, C_S, is known to be

$$C_s = \varepsilon_0 \varepsilon_r \frac{A}{d} \qquad (2\text{-}2)$$

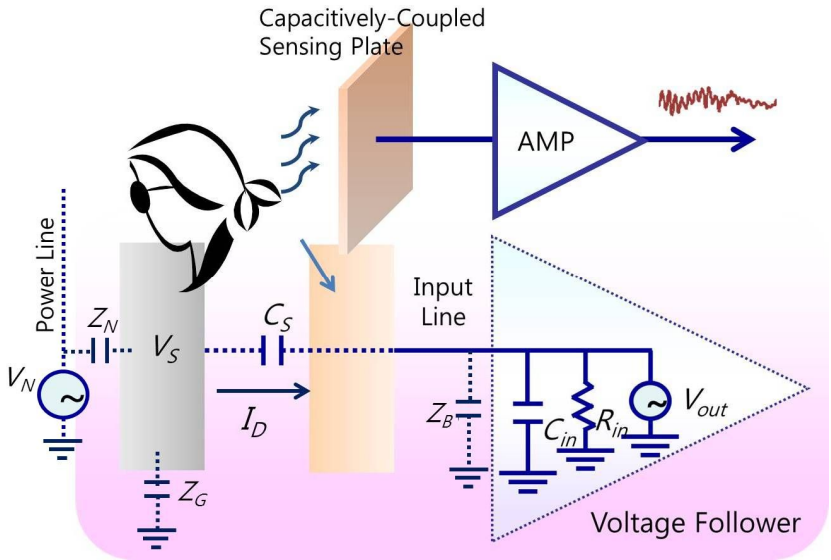

Figure 2-1. Diagram for capacitively-coupled measurement of the EEG.

where A is the area of the electrode surface, d is the distance between the scalp and the electrode surface, ε_0 is the vacuum permittivity and ε_r is the dielectric constant of the hair. For a high coupling capacitance, a large electrode size with strong optimal contact for small and unchanged thickness between electrode and scalp is essential. This can be also described in reverse: that the input capacitance, C_{in}, should be substantially smaller than the coupling capacitance, C_S. The input resistance should also be larger than $1/\omega C_s$, according to equation (2-1). Therefore, a capacitively-coupled electrode should be designed to make electrode input impedance very high. In practice, hair cannot be regarded as a pure capacitor. I have

observed results that can be explained by the introduction of conductance (R_S). From my observations, impedance depends heavily on moisture.

In conclusion, because of the very small source capacitance, C_S, designing a very high input impedance amplifier as well as the amplifier's bias network is challenging for the front ends of capacitively-coupled EEG electrodes. Impedance between the body and the power line (Z_N), body and ground (Z_G) should be considered for effective common mode noise cancellation. Capacitance between the input (the electrode face and input line pattern) and the ground of the amplifier (Z_B) also should be considered for noise minimization. In this study, direct grounding at the exposed bare skin of the forehead was employed for reducing external noise. Based on the above electronic model, high input impedance active electrodes for BCI applications were investigated.

2.1. Pre-amplifier Topologies

Figure 2-2 shows the structure of the tested electrodes, which consists of an electrode face, pre-amplifier, and shielding plate. The electrode was designed as a circular plate (D: 36mm), made of PCB clad with copper and plated with gold. The shield was made of aluminum as a case surrounding the rear of the electrode with a height of 11.71mm from the electrode face, (figure 2-2). The pre-amplifier circuit was printed on the backside of the electrode. Four kinds of pre-amplifier circuit were tested in this study. In figure 2-3, R_s and C_s represent the resistance and capacitance, respectively, of the hair between the electrode face and scalp. R_a and C_a denote the input resistance and capacitance, respectively, of the pre-amplifier. Figure 2-3 (a) shows the front end of a capacitively-coupled EEG electrode, which basically consists of a voltage follower. An op-amp (OPA124, Texas Instruments) with an input resistance of $10^{13}\Omega$ and input capacitance of 1 pF was used in the pre-amplifier. R_b is a resistor for the bias current of the op-amp. The bias resistor R_b should be grounded with very high value resistance in order to avoid degrading input impedance and reducing output noise. The maximum R_b value is generally on the order of Tera (10^{12}) Ω with regard to amplifier bias current and power supply voltage. However, a 50GΩ bias resistor was used in this study. The bias resistor value affects low frequency gain and cutoff frequency. Since a relatively low R_b value was

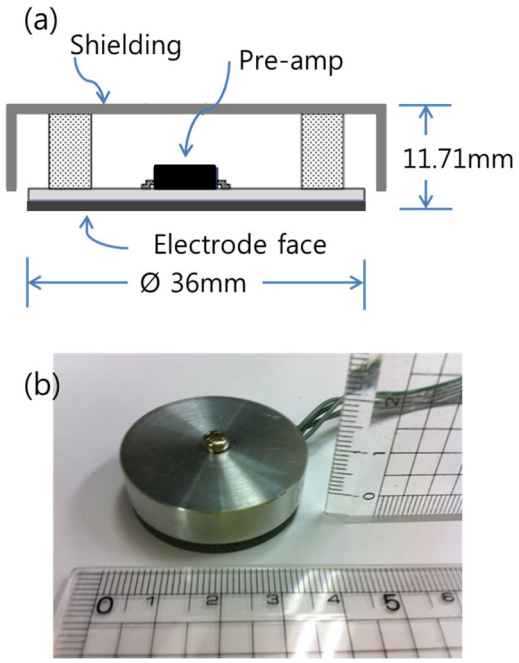

Figure 2-2. Prototype of the capacitively-coupled EEG electrode: (a) cross-sectional configuration of the active electrode, (b) photograph of the active electrode.

employed in this study, the signal low cutoff frequency was several hertz and the amplifier gain was strongly dependent on coupling capacitance. This combination can introduce low frequency distortion of the EEG and limits diagnostic capability. However, the electrode can monitor sufficient EEG signals for BCI applications.

In figure 2-3 (b), active guarding involving positive feedback was added to the basic voltage follower scheme. This feedback reduces the effects of stray capacitances between the electrode and the shielding plate. Active guarding is implemented by

surrounding the electrodes with shielding cases that are driven to the same node potentials by low output impedance circuits with feedback gain. In this way, no potential differences appear on both sides of the stray capacitance. Figure 2-3 (c) and (d) describe how the requirement for an ultrahigh value bias resistor may be eliminated [38, 39]. In figure 2-3 (c), two low leakage anti-parallel diodes, $D_{1,2}$, are employed to achieve an R_b value on the order of TΩ. The use of diodes ensures that amplifier bias is set to V_{ref} while the bootstrap maintains the dynamical voltage across diodes near zero.

As a result, the leakage across the diode remains very small and noise contributions are minimal, while effective electrode input impedance becomes very high. In figure 2-3 (d), an INA116 (Burr-Brown Corporation) was employed as a high input impedance pre-amplifier and reliably charged a floating input to a point within the allowable input range shortly after power-up purely through leakage currents, removing the need for an external bias network. Signals from the non-inverting input guard were connected to the inverting input to remove drift and DC offset. Positive feedback, adjusted by R_3, was used to ensure the unit gain of the electrodes.

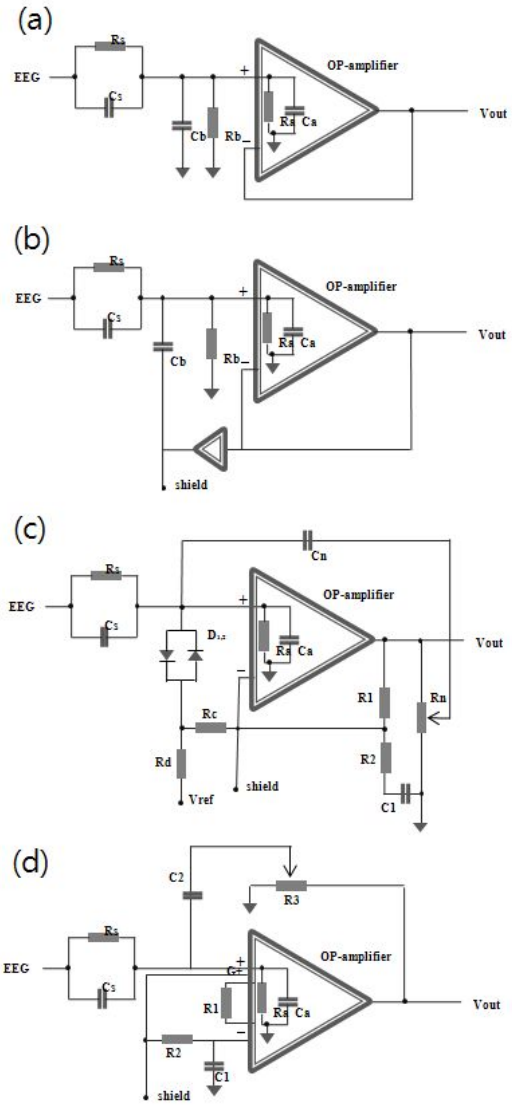

Figure 2-3. Schematics of the capacitively-coupled EEG electrodes tested in this study. (a) Basic voltage follower scheme with high value resistor bias network, (b) voltage follower scheme with active guarding, (c) reverse current of signal diodes to provide bias current [38], (d) electrode scheme without any external bias network [39].

2.1.1. Frequency Responses

The frequency responses of the electrodes were experimentally measured in a simulated environment using sinusoidal wave frequency sweep. Experiments were performed using the same method used in our previous study [40-42]. A wig of real human hair was employed as an insulator instead of cloth for simulations. A copper plate (20cm x 20cm) was laid on a table, connected to a function generator, and then covered with the wig. A capacitively-coupled EEG electrode was placed on the wig, and then pressed with a pressure of about 800N/m^2 by a weight placed on the electrode. Figure 2-4 shows the frequency responses of the tested electrodes. The obtained frequency responses show the relatively low voltage gain and large phase difference in very low frequency range, and these are similar to those presented by *Chi et al*., who tested electrode (c) and (d) [38, 39]. However, stable gain responses and small phase differences were obtained in the frequency range of interest (4-100Hz) for BCI applications. Although small gain and some phase differences existed below 4Hz, clear sinusoidal waveforms were measured using the tested electrodes except for electrode (c). Severe waveform distortion was observed below 4Hz for electrode (c). (experimental data below 4Hz for electrode type (c) in figure 2-4 and 5 are represented by the gray line).

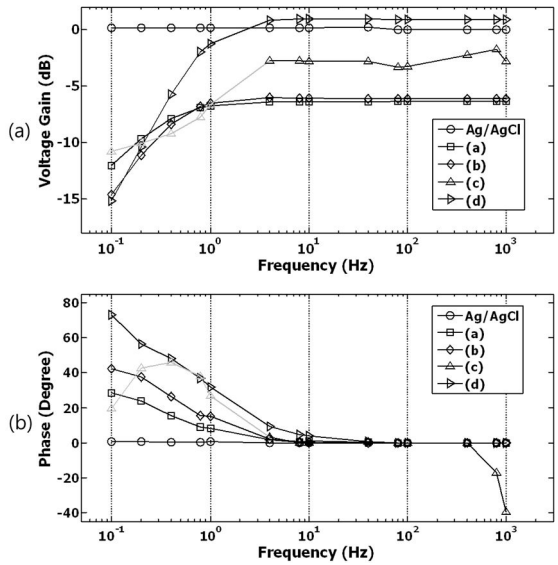

Figure 2-4. Frequency response of the capacitively-coupled EEG electrode through real human hair: (a) voltage gain, (b) phase difference.

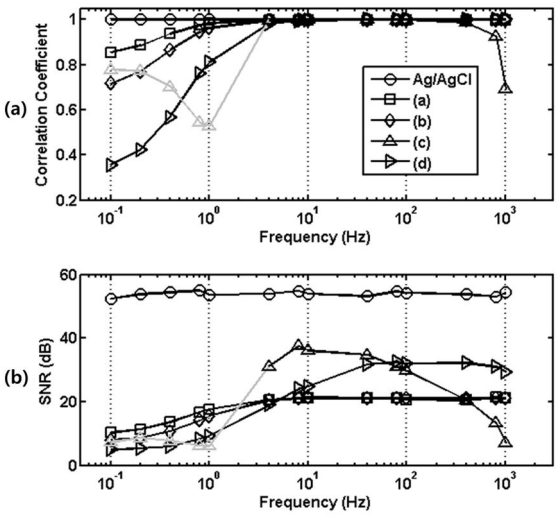

Figure 2-5. Quantitative analysis of the tested electrodes (wet electrode, capacitively-coupled electrode (a), (b), (c), (d)). Subplot (1): correlation coefficients, subplot (b): signal to noise ratio.

Figurre 2-5 shows the results of quantitative analysis using measured signals. Correlation coefficients between the original clean sinusoidal wave generated from the function generator and those measured by electrodes shows reasonable values (>0.99) in the frequency range of interest (4-100Hz) for all electrodes (Figure 2-5 (a)). However, marked differences are noted in the correlation coefficient value in the low frequency range, especially for the capacitively-coupled electrode (c) due to phase differences. Electrode (c) also shows a decreased correlation value (0.69) at 1000Hz. Figure 2-5 (b) shows the signal-to-noise ratio (SNR) for all electrodes over frequency range from 0.1 to 1000Hz. The SNRs were calculated using normalized signals that have a maximum value of 1V in order to investigate the amount of noise in capacitively-coupled measurements. Electrodes (a) and (b) show relatively small changes in SNR values, especially for the frequency range above 4Hz. Although electrodes (c) and (d) show relatively higher SNR values in the frequency range between 10 and 100Hz than seen with electrodes (a) and (b), they show large differences in SNRs according to the measured frequency band. In addition, electrode (c) shows the lowest SNR value among the tested electrodes in the frequency of 800Hz (13.20dB) and 1000Hz (7.13dB).

2.1.2. Signal Comparison with a Conventional Wet Electrode

For this experiment, the capacitively-coupled electrode and a conventional wet electrode (Gold-disk cup electrode, Grass Technology, West Warwick, RI, USA) with conduction paste were placed at neighboring positions of *O2* and *C4* for comparisons. Figure 2-6 shows simultaneous EEG recordings obtained with the conventional and capacitively-coupled electrodes. Table 2-1 shows correlation coefficients between time series EEG signals measured by both types of electrodes on five subjects. The average correlation coefficients between standard and capacitively-coupled electrodes over the five subjects were 0.795, 0.795, 0.633, and 0.655 for each capacitively-coupled electrode at *O2* and 0.843, 0.782, 0.625, and 0.543 for each capacitively-coupled electrode at *C4*. Although measurements were performed at neighboring sites, their exact positions were different. In addition, the relatively large areas of the capacitively-coupled electrode caused a spatial averaging effect on the measured signal. Considering these measurement conditions, the resulting correlation coefficients were acceptable for the validation of the presented electrodes. The EEG signals shown in Figure 2-6 suggest that capacitively-coupled EEG measurements conform to EEG measurements using conventional electrodes.

Therefore, the EEG signals recorded by paste-based and capacitively-coupled electrodes were similar. Although capacitively measured EEG signals may not be used for clinical situations and medical applications, they are sufficient for non-medical purposes such as BCI applications.

Table 2-1. Correlation coefficients between EEG signals measured using standard wet electrode and capacitively-coupled electrodes in five subjects

O_2	(a)	(b)	(c)	(d)
A	0.778	0.759	0.631	0.703
B	0.814	0.784	0.573	0.607
C	0.709	0.676	0.588	0.607
D	0.835	0.836	0.749	0.639
E	0.838	0.892	0.626	0.720
mean	0.795	0.795	0.633	0.655

C_4	(a)	(b)	(c)	(d)
A	0.879	0.653	0.622	0.431
B	0.827	0.710	0.779	0.662
C	0.840	0.796	0.742	0.591
D	0.824	0.849	0.336	0.532
E	0.846	0.904	0.648	0.497
mean	0.843	0.782	0.625	0.543

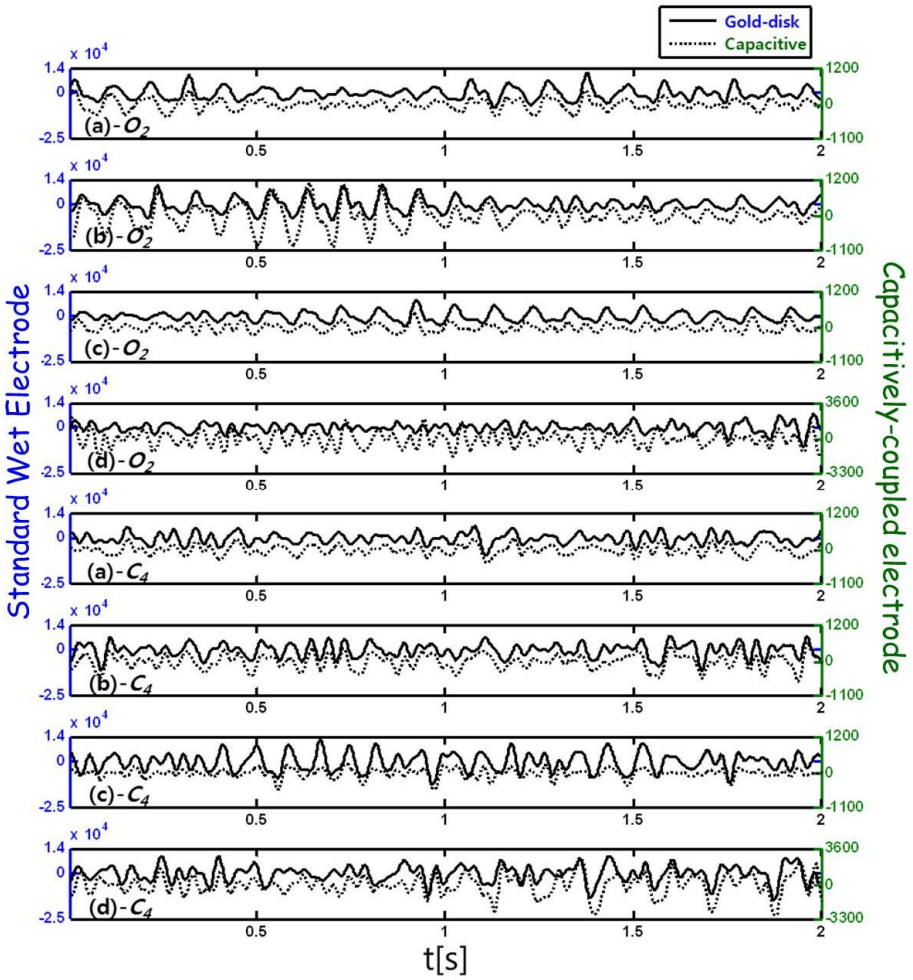

Figure 2-6. Comparison of the EEG signal measured using standard wet electrode (solid line) and capacitively-coupled electrode (a), (b), (c), (d) (dashed line) at neighboring position of O_2 (upper four plots) and C_4 (lower four plots).

2.2 Active Electrode for Capacitively-coupled EEG Measurement

Based on the results in section 2.1, a voltage follower scheme with a high value bias resistor was selected for further study. Figure 2-7 shows a diagram of the selected capacitively-coupled electrode including the electrode-scalp interface model (Z_{HAIR}). A capacitively-coupled electrode basically consists of an AC-coupled voltage follower. Because of its very small coupling capacitance, C_{HAIR}, designing an active electrode with ultra-high input impedance is challenging. In addition, a stable path for the bias current of the operational amplifier (op-amp) should be provided. Due to these requirements, the inclusion of an ultra-high-value grounded resistor, R_B, is accepted in capacitively-coupled biopotential measurement. The parallel connection of C_{HAIR} and R_{HAIR} represents electrode impedance between the electrode surface and the scalp. C_{HAIR} is determined by the dielectric property and thickness of the hair (distance between scalp and electrode surface), as well as the effective electrode area. Several reports have described conductance that depended heavily on moisture in capacitively-coupled biopotential measurements; therefore, hair cannot be regarded as a pure capacitor with regard to sweat for long-term use. Based on the capacitively-coupled EEG measurement model presented in Figure 2-7, the voltage gain, G_S, for

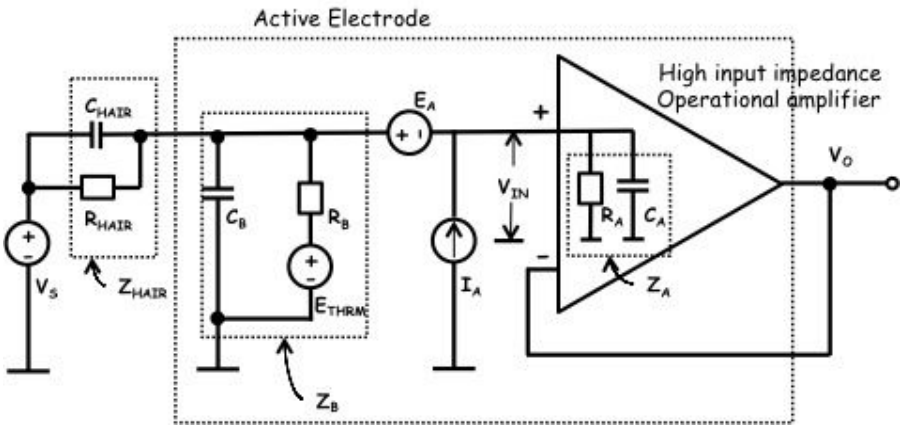

Figure 2-7. Diagram of the capacitively-coupled electrode model, including the electrode-scalp interface model (Z_{HAIR}).

the V_S (EEG source) can be expressed as in Equation (2-3). The input impedance Z_A should be sufficiently large to be disregarded in comparison with Z_B.

$$G_S = \frac{V_O}{V_S} = \frac{Z_B // Z_A}{Z_{HAIR} + Z_B // Z_A} \cong \frac{R_B + C_{HAIR} R_B R_{HAIR} s}{(R_B + R_{HAIR}) + (C_B + C_{HAIR}) R_B R_{HAIR} s} \quad (2\text{-}3)$$

If we consider the intrinsic noise of the op-amp to be represented by a voltage noise source E_A and current noise source, I_A, the bias resistor's thermal noise source, E_B, and noise from the resistance of the hair, E_{HAIR}, then the measured output signal can

be calculated as in Equation (2-4) and the signal to noise ratio (SNR) can be expressed as in Equation (2-5).

$$V_O = G_1 V_S + G_2 I_A + G_3 E_A + G_4 E_{THRM}, \qquad E_{THRM} = \sqrt{4kTBR_B} \tag{2-4}$$

where, k = Boltzmann's constant, T = absolute temperature, and B = noise bandwidth.

$$SNR = \frac{|V_S|}{\sqrt{I_A^2 |Z_{HAIR}|^2 + E_A^2 \left|1 + Z_{HAIR}(j\omega C_B + \frac{1}{R_B})\right|^2 + E_{THRM}^2 \left|\frac{Z_{HAIR}}{R_B}\right|^2}} \tag{2-5}$$

Impedance between the scalp and the surface of the capacitively-coupled electrode (Z_{HAIR}) is high compared with that of conventional direct contact electrodes because of the insulating effect of hair. Equations (2-3) and (2-5) indicate that in order to measure the signal using capacitance, we should increase the resistance R_B and reduce the electrode impedance Z_{HAIR}; resistances from hundreds of giga-ohms to tera-ohms are now easily available. In order to reduce the electrode's impedance, we should maximize its coupling capacitance. Since coupling capacitance is proportional

to the contact area of an electrode, a conventional rigid-surfaced electrode has limited performance in terms of figure 1-4, especially for EEG measurement.

2.3 The Foam-surfaced Capacitively-coupled Electrode

Figure 2-8 shows the profile of the capacitively-coupled electrode with the soft dry conductive foam surface. The electrode was composed of an embedded pre-amplifier, shielding block and electrode face with dry foam surface adaptive to head topography (Conductive Cushion-TRO, A-Jin Electron, Busan, Korea). The electrode was designed as a circular plate made of PCB clad with copper and plated with gold. The conductive foam was applied onto this exposed gold substrate to provide a cushioning effect. The surface of the electrode was fabricated of polyolefine covered by polyurethane. The foam was coated with Ni/Cu on all surfaces to establish an electrical conduction similar to other dry electrodes. There are conduction holes providing electrical conductance between the upper and lower layers of the foam material. Its conductance (sheet resistance) is about 0.08 Ω/sq for surface resistance and 0.03 Ω/sq for top-down resistance. The shield was made as an electrode case that surrounded the rear of the electrode. It was made of aluminum with a height of 11.71 mm from the bare electrode face. The thickness of the foam material was 1.2 mm and the final construction for the electrode application was made by stacking five layers

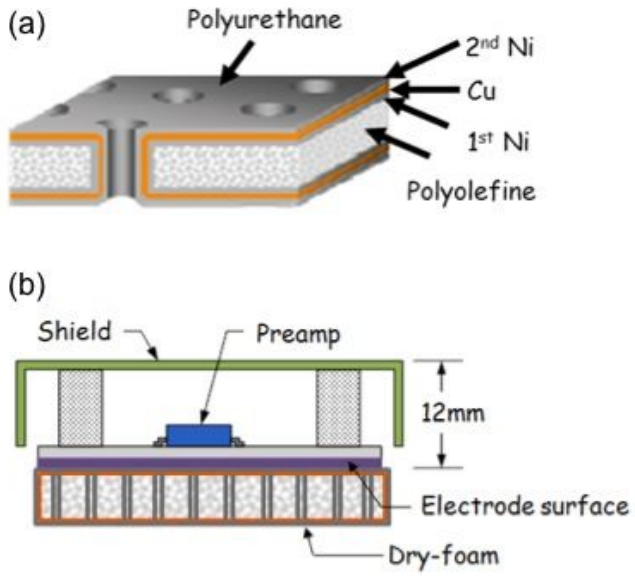

Figure 2-8. Configuration of (a) the foam material used and (b) the proposed foam-surfaced capacitively-coupled electrode.

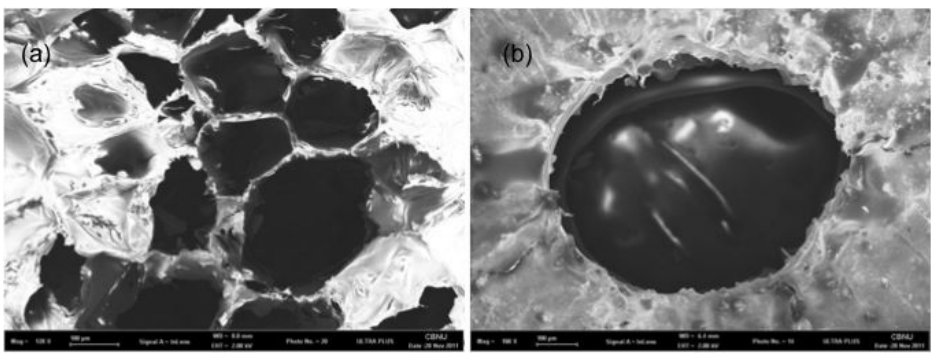

Figure 2-9. SEM images of (a) cross-sectional view and (b) surface view of the conductive foam. Closed pores ensure its cushioning ability and surface holes ensure electrical conductance for the entire foam area.

together, yielding a final size for the proposed electrode of 36 mm in diameter by 17.71 mm in height. The scanning electron microscope (SEM) images of the applied foam are presented in figure 2-9. Figure 2-9(a) shows a cross-sectional image of the foam and indicates its cushioning ability with closed pores. Figure 2-9(b) shows how the surface of the material and its holes provide electrical conduction for the entire area of the foam material. This soft foam guarantees intimate contact between the hairy scalp surface and the capacitively-coupled electrode.

In summary, the final construction of the foam-surfaced capacitively-coupled electrode is illustrated in figure 2-10. It consists of an electrode facade with polymer foam conforming to head topography, an embedded pre-amplifier, and a shielding box. The electrode was designed as a circular plate 36mm in diameter and 17.71mm in height (including the height of the foam material and shielding box). The shielding box, made of aluminum, was grounded and placed at the rear of the electrode. The foam consisted of polyolefine covered by polyurethane and coated with Ni/Cu to allow for electrical conductance. Between the upper and lower layers of foam material, sparse vertical holes were created to allow for electrical conductance throughout the entire foam area.

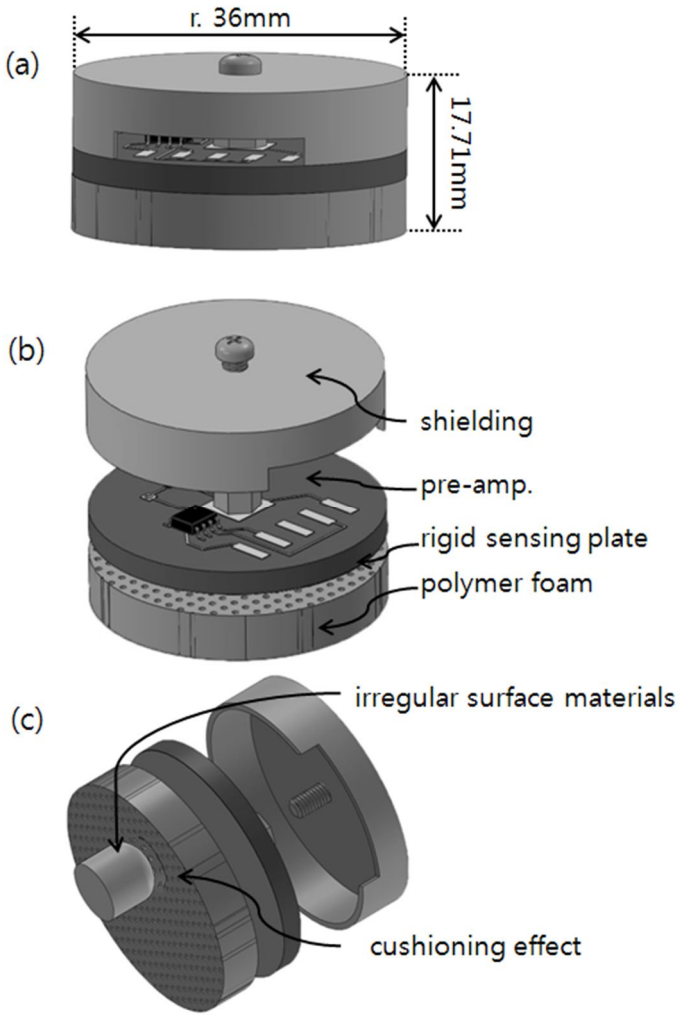

Figure 2-10. Three-dimensional drawing of the polymer foam-based capacitively-coupled EEG electrode design: (a) lateral view with dimensional specifications, (b) trimetric view demonstrating physical composition, (c) conceptual drawing demonstrating how the polymer foam adapts to irregular surface material such as hair or head topography. Note that irregular surface material in this figure was simplified for clarity.

2.3.1. Impedance Spectroscopy

The electrode surface-skin contact impedance was investigated using an SI 1260 impedance analyzer (Solartron Analytical, Farnborough, UK) with a 1294 impedance interface (Solartron Analytical) for safety. A standard gel-type electrode (3M Red Dot foam monitoring electrode 2225 (Ag/AgCl), 3M Health Care, St. Paul, MN, USA), a conventional rigid-surfaced capacitively-coupled electrode and our proposed dry foam-surfaced capacitively-coupled electrode were tested for comparison. In order to investigate the effect of the foam surface on contact impedance, a hairy and a hairless site were selected for the experiments. The test electrode was placed with constant pressure on a test subject's hairless forearm and hairy ankle sites using a Velcro strap and was exchanged carefully between each measurement to avoid any change in the skin surface. For each test electrode, impedance measurements were carried out soon after applying the electrode. Impedance was measured according to the change in frequency from 0.1 Hz to 1 KHz.

2.3.2. Frequency Responses

To assess the actual frequency response of the proposed electrode with regard to hair, a means of measuring the frequency response of the electrode was designed. It was experimentally measured by simulating the environment using a sinusoidal wave frequency sweep. In this experiment, a wig made of real human hair was employed as an insulator to simulate an actual situation: the irregular surface between the electrode and the scalp. A copper plate (20 cm x 20 cm) was laid on a table, connected to a function generator, and then covered with the wig. A conventional capacitive electrode and the proposed soft foam electrode were placed on the wig, and pressed into it with a pressure of about 800 N/m^2 by a weight placed on the electrode. The Ag/AgCl electrode employed in the impedance experiment was also placed directly on the copper plate. A sinusoidal signal of 1 V peak to peak was applied, and the frequency was swept between 0.1 Hz and 1 kHz. The signals measured using the three kinds of electrodes were digitized using a Biopac MP150 (Biopac Systems Inc., Goleta, CA, USA) and the signal from the function generator was also directly digitized as a reference. The voltage gain and phase difference were then calculated with regard to the sinusoidal wave frequency.

2.3.3. Signal-to-Noise Ratio and Signal-to-Error Ratio

The signal quality was investigated by analyzing the SNR and signal-to-error ratio (SER) [43]. For this, a realistic simulation environment was made using a human head model that was electrically conductive, covered with real human hair, and connected to an EEG simulator (Model EEGSIM, Grass Technology, West Warwick, RI, USA). Although the human head model employed in this study was totally conductive and therefore, only one-channel EEG could be applied to the head model, quantitative evaluations could be performed since the original clean EEG signal generated from EEG simulator and those measured capacitively through the hair could be directly assessed. The amount of noise in a capacitively measured EEG signal is assessed by SNR:

$$SNR = \frac{\sum_{t=0}^{L-1} x^2(t)}{\sum_{t=0}^{L-1} n^2(t)}, \qquad \text{(2-6)}$$

where $x(t)$ is the original clean reference EEG signal directly recorded from the simulator and $n(t)$ is the measured noise realization. The quantitative evaluation for the capacitively measured EEG signal is also assessed by SER:

$$SER = \frac{\sum_{t=0}^{L-1} x^2(t)}{\sum_{t=0}^{L-1} [x(t) - \hat{x}(t)]^2}, \quad (2\text{-}7)$$

where $\hat{x}(t)$ is the capacitively measured EEG signal. The proposed dry foam-surfaced capacitively-coupled electrode was compared with a conventional rigid-surfaced capacitively-coupled electrode. The SNR was calculated using normalized EEG signals measured from the capacitively-coupled electrodes and also using those in which the power line noise (60 Hz) was removed. SER was calculated using both raw signals and normalized signals, since the capacitively-coupled measurement of EEG provided diminished amplitude signals compared to conventional resistively-coupled measurement. The EEG data were normalized to have a maximum value of 1V. The original simulated EEG data and capacitively measured data using the conventional rigid-surfaced and proposed foam-surfaced electrodes were simultaneously measured over five minutes for each trial, and a total of ten trials were performed for SNR and SER analysis.

2.4 EEG Measurement without Conductive Contact

2.4.1. Common-mode Interference Rejection

Figure 2-11 (a) shows the schematic circuit for capacitive EEG measurement using monopolar leading. One capacitively-coupled electrode (active) is placed over hair and the reference electrode (silent), as well as third electrode (driven), is placed directly on the skin. Conditions for bipolar EEG are illustrated in Figures 2-11 (b) and (c). The capacitively-coupled electrode pair (active) is located over hair and the third electrode (driven) can be placed directly on the skin (b) or over hair (c). The following four equations can be derived using Kirchhoff's current (KCL) and voltage law (KVL) from equivalent circuit presented in Figure 2-12.

$$sC_P(V_P - V_{CM} - V_G) = sC_B(V_{CM} + V_G) + sC_S V_G \qquad \text{(2-8-a,b,c)}$$

$$sC_S V_G = \frac{V_{CM} + A(V_{C1} + V_{C2})}{R_{E3}} + sC_{E1}(V_{CM} - V_{C1}) + \frac{(V_{CM} - V_{C2})}{R_{E2}} \qquad \text{(2-9-a)}$$

$$sC_S V_G = \frac{V_{CM} + A(V_{C1} + V_{C2})}{R_{E3}} + sC_{E1}(V_{CM} - V_{C1}) + sC_{E2}[(V_{CM} - V_{C2})] \qquad \text{(2-9-b)}$$

$$sC_S V_G = sC_{E3}[V_{CM} + A(V_{C1} + V_{C2})] + sC_{E1}(V_{CM} - V_{C1}) + sC_{E2}(V_{CM} - V_{C2}) \qquad \text{(2-9-c)}$$

$$sC_{E1}(V_{CM}-V_{C1})=\frac{V_{C1}}{[Z_B // Z_{in1} // Z_{in2}]} \quad \text{(2-10-a,b,c)}$$

$$\frac{(V_{CM}-V_{C2})}{R_{E2}}=\frac{V_{C2}}{Z_{in2}} \quad \text{(2-11-a)}$$

$$sC_{E2}(V_{CM}-V_{C2})=\frac{V_{C2}}{[Z_B // Z_{in1} // Z_{in2}]} \quad \text{(2-11-b,c)}$$

Solving the above equations, the transfer function between common mode voltage, V_{CM} and external noise source, V_P can be obtained:

$$\frac{V_{CM}}{V_P}=\frac{C_P}{C_P+C_B+(C_B+C_S+C_P)K} \quad \text{(2-12)}$$

where,

$$K=\frac{1}{sC_SR_{E3}}+\frac{AC_{E1}X}{C_SR_{E3}(1+sC_{E1}X)}+\frac{AY}{sC_SR_{E3}(R_{E2}+Y)}+\frac{C_{E1}}{C_S}-\frac{sC_{E1}^2X}{C_S(1+sC_{E1}X)}+\frac{1}{sC_SR_{E2}}-\frac{Y}{sC_SR_{E2}(R_{E2}+Y)} \quad \text{(2-13-a)}$$

$$K=\frac{1}{sC_SR_{E3}}+\frac{AC_{E1}X}{C_SR_{E3}(1+sC_{E1}X)}+\frac{AC_{E2}Y}{C_SR_{E3}(1+sC_{E2}Y)}+\frac{C_{E1}}{C_S}-\frac{sC_{E1}^2X}{C_S(1+sC_{E1}X)}+\frac{C_{E2}}{C_S}-\frac{sC_{E2}^2Y}{C_S(1+sC_{E2}Y)} \quad \text{(2-13-b)}$$

$$K=\frac{C_{E3}}{C_S}+\frac{AC_{E3}(sC_{E1}X)}{C_S(1+sC_{E1}X)}+\frac{AC_{E3}(sC_{E2}Y)}{C_S(1+sC_{E2}Y)}+\frac{C_{E1}}{C_S}-\frac{sC_{E1}^2X}{C_S(1+sC_{E1}X)}+\frac{C_{E2}}{C_S}-\frac{sC_{E2}^2Y}{C_S(1+sC_{E2}Y)} \quad \text{(2-13-c)}$$

$$X=[Z_B // Z_{in1} // Z_{in2}] \quad \text{(2-14-a,b,c)}$$

$$Y=[Z_{in1}] \quad \text{(2-15-a)}$$

$$Y=[Z_B // Z_{in1} // Z_{in2}] \quad \text{(2-15-b,c)}$$

Unknown values and parameters were assumed like below from related literature [44-46]:

$Z_{in1} : 10^{10}\Omega // 4pF$; input impedance of INA118 (Burr-Brown)

$Z_{in1} : 100T\Omega // 3pF$; input impedance of OPA124 (TI)

$Z_B : 50G\Omega // 18pF$; bias resistor and input path capacitance

$C_P : 2pF$, $C_B : 200pF$, $C_S : 200pF$

$C_{E1} : 33pF$, $R_{E2} : 100k\Omega$, $R_{E3} : 100k\Omega$

Finally, the EEG signal was measured while the subject performed an eye opening/closing task to extract the alpha wave.

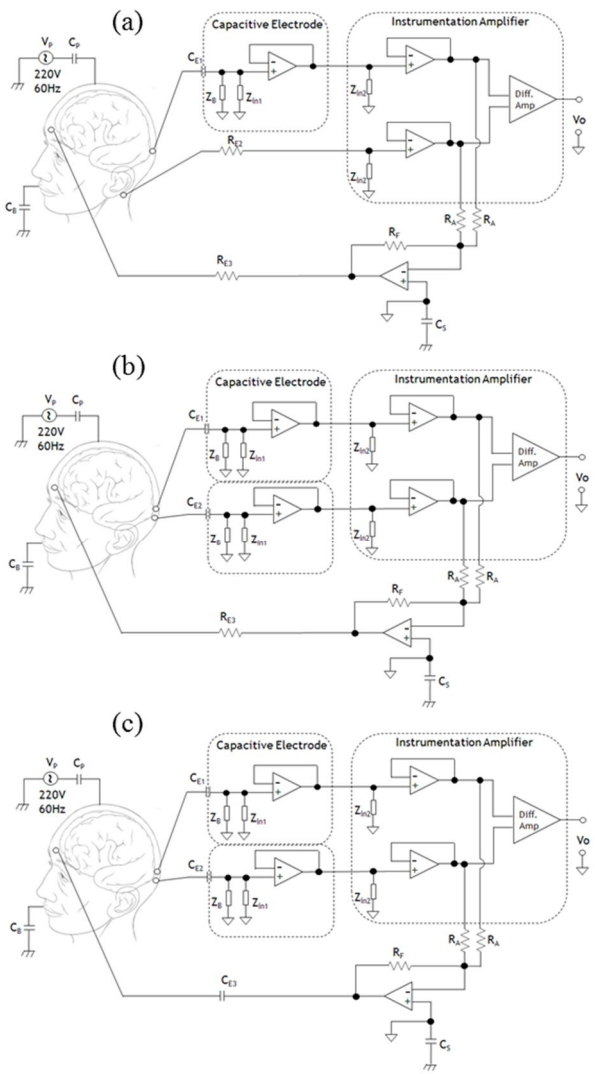

Figure 2-11. Schematics of the Driven-Right-Leg (DRL) circuit application for capacitively-coupled measurement of EEG: (a) capacitively-coupled monopolar leading with resistive reference and driven, (b) capacitively-coupled bipolar leading with resistive driven and (c) full capacitively-coupled bipolar leading.

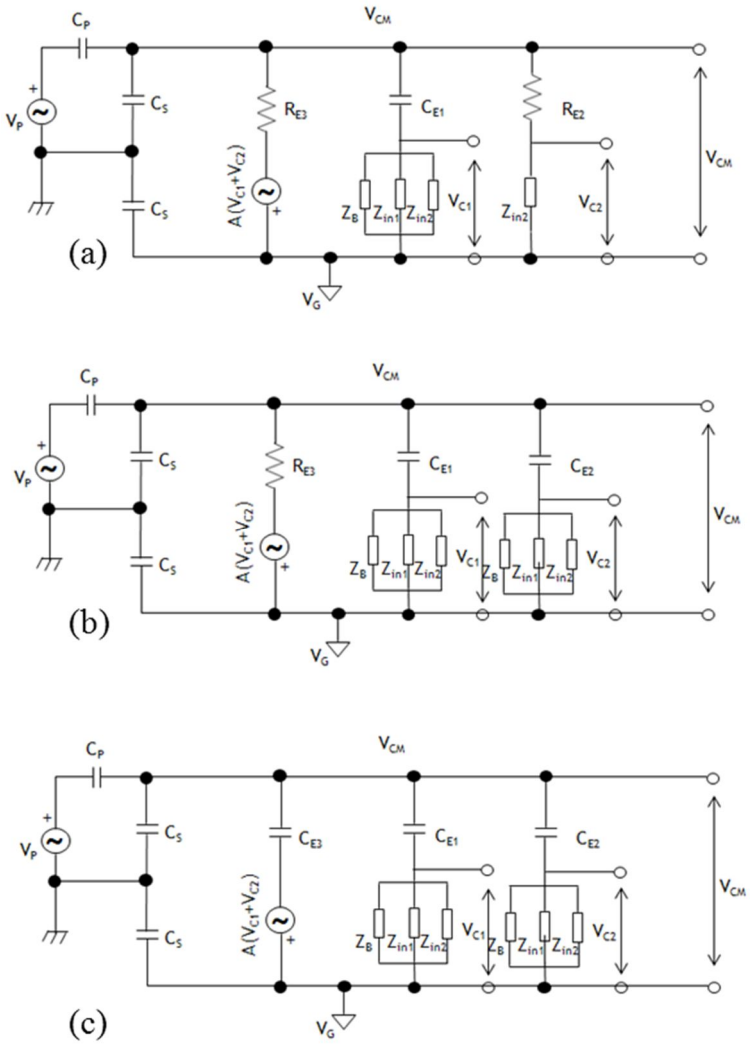

Figure 2-12. Equivalent electronic circuits for figure 2-11.

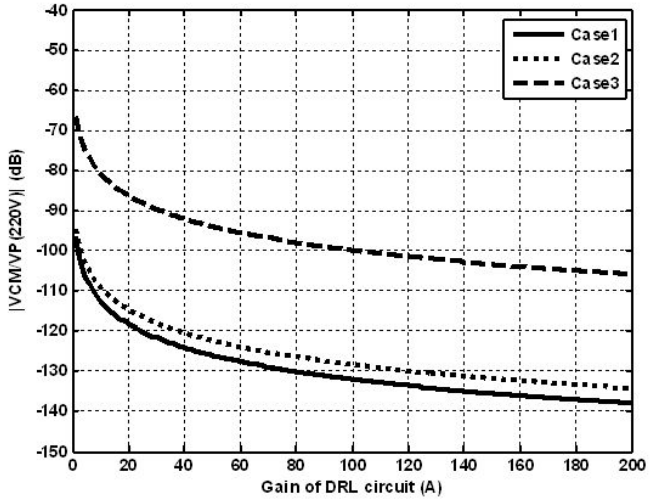

Figure 2-13. Gain response for common mode interference suppression (f=60Hz): *(solid line)* capacitively-coupled monopolar leading with resistive reference and driven, *(dotted line)* capacitively-coupled bipolar leading with resistive driven and *(dashed line)* full capacitive-coupled bipolar leading.

Figure 2-13 shows the gain response for the common mode interference suppression for f=60Hz. In this figure, negative feedback is not working and the isolated common is connected to third electrode if the gain (A) is 0. When the third electrode was placed directly on the skin, the common mode rejection was considered to be greatly reduced, so that even DRL is not working (case 1 and 2 at zero gain in figure 2-13; direct grounding). However, common mode interference still remains when the third electrode is located over hair (case 3 in figure 2-13). In order to

provide similar common mode interference suppression performance in full capacitively-coupled configuration with those in direct skin grounding (case 1 and 2 at zero gain in figure 2-13), a gain of about 100 is needed.

Figure 2-14 shows the EEG signals measured under the three measurement conditions described in figure 2-11. The upper signal of each subplot shows the EEG when the third electrode was connected to the isolated amplifier common and the lower signal of each subplot shows the EEG while the DRL circuit drives the third electrode through a feedback loop with a gain of 200. For all measurements, the subject was instructed to open or close his eye according the verbal instruction of experimenter. The illustrated signal in figure 2-14 is 4 seconds long. The earlier 2 seconds were recorded while the subject opened his eye (gray color) and the later 2 seconds were recorded while the subject closed his eye (black color). Clear alpha activities can be observed in the (a) and (b) conditions regardless of DRL application; however, SNR is much more improved with the DRL. For the (c) condition, the signal was significantly corrupted by common mode interference; therefore, the EEG signal cannot be determined using a third electrode connected to the amplifier's ground (upper signal in figure 2-14 (c)). However, the SNR was dramatically increased by driving the third electrode through a negative feedback loop with a gain, as shown in the lower signal of figure 2-14 (c). The EEG signal measured using DRL

circuitry is known always to provide a higher SNR compared with signals measured using a third electrode connected to the amplifier common. However, when the third electrode was placed directly on the skiny, the connection of the third electrode to the amplifier common also enabled EEG acquisition of reasonable quality for non-clinical purposes [47].

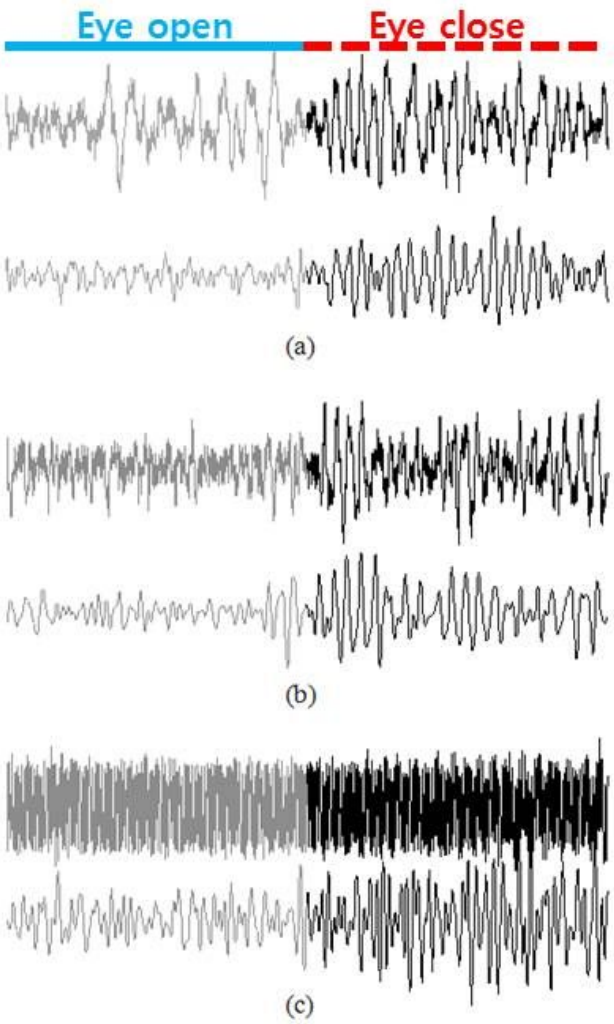

Figure 2-14. The EEG signal measured under the three different circuitry conditions illustrated in figure 2-11. The upper signal of each subplot shows EEG when the third electrode was connected to amplifier common and the lower signal of each plot shows EEG when the third electrode was connected to negative feedback loop for DRL application. The EEG depicted in gray tone is the opened eye and that in black is the closed eye periods.

2.4.2. EEG Measurement over Hair

Five volunteers (all males aged from 26 to 30), who had no history of neurological disease and no neuropathological abnormalities, consented to participate in testing of the newly proposed electrode by means of a number of experiments. Spontaneous EEG waves were recorded to compare the performance of the standard wet electrodes with the capacitively-coupled electrodes. Capacitively measured EEG signals were directly compared with the EEG signals measured using a reference standard wet electrode (Gold-disk cup electrode, Grass Technology, West Warwick, RI, USA) with conduction paste. The reference wet electrode, conventional rigid-surfaced capacitively-coupled electrode and proposed foam-surfaced capacitively-coupled electrode were placed in a triad over O_2 and C_4, as closely together as possible in order to compare them. This placement enabled us to perform simultaneous recording with the resistively-coupled (paste-based) and capacitively-coupled electrodes (conventional rigid-surface-based and proposed foam-surface-based) at close locations. The EEG conduction paste used in this study was Elefix (Nihon Kohden, Tokyo, Japan). Capacitively-coupled electrodes were mounted on the scalp hair without any skin preparation or electrolyte application. The relative placement of the electrodes was consistent between different subjects. Care was taken to prevent EEG

conduction paste from the wet electrode from seeping into the neighboring capacitively-coupled electrodes. All EEG signals were measured with a reference electrode at A_2 and grounding electrode at *Fpz*. These two electrodes were not capacitively-coupled; dry electrodes that do not require conduction gel or paste were employed. The EEG signals from the electrodes were transmitted through a lab-made hardware module composed of a high-pass filter (0.05 Hz), low-pass filter (30 Hz) and 60-Hz notch filter and an amplifier. The EEG signals were digitized at a sampling rate of 512 Hz using an analog-to-digital converter (NI-DAQ Pad 6015, National Instruments Co., Austin, TX, USA) and recorded using a BCI2000 general purpose software platform developed by the BCI research group at the Wadsworth Center, USA [15]. The BCI2000 data files were analyzed using a Matlab MEX file that is included with the BCI2000 distribution package. Finally, subjects were asked to open and close their eyes for purposes of EEG alpha rhythm comparisons. Figures for the EEG measurement results of subject 1 only are presented in this paper.

2.5. BCI Experiments

2.5.1. Steady-State Visual Evoked Potential-based BCI

The Bremen BCI paradigm, which is well known and widely used for SSVEP-based BCI studies was employed [48-50]. Stimuli were generated using Matlab with Psychotoolbox, and presented on a 19" flat screen monitor (FLATRON Slim, LG Electronics Ltd., Korea). The five checkerboard patterns at the outer edges and center of the screen flickered at 12, 7.5, 8.57, 6.67 and 5.45 Hz and corresponded to the commands "LEFT (L)", "UP (U)", "RIGHT (R)", "DOWN (D)" and "SELECT (S)" respectively. Although the original Bremen BCI interface provides 32 characters and stimuli in the same screen, additional screens were employed for experimental convenience. The graphical user interface was presented in a second screen next to the stimulus screen. At the beginning of each run, a cursor appeared over the "E" character. Subjects could navigate the cursor to the desired character by gazing at one of the four directional commands or choosing the character directly. After making a selection command, the cursor automatically moved back to the "E" character therefore, at least 12 commands were required in order to spell the word "BRAIN" (D→R→S→D→S→L→L→S→U→S→L→S).

Subjects were seated in a comfortable chair approximately 60cm away from the LCD screen. They wore a capacitively-coupled electrode cap consisting of two capacitively-coupled electrodes attached to an O_1 and O_2 site on a normal baseball cap (see Figure 2-15 (a)). EEG data were recorded using a reference electrode at A_2 and ground electrode at F_{pz}. Subjects performed offline experiments first in order to optimize the analysis window size. Participants were then asked to gaze at each stimulus for 10s, in a random fashion according to verbal instructions provided by the experimenter. This process was repeated 10 times; therefore, 10 sets of five SSVEP epochs were collected. In the offline experiments, no feedback was given to the subjects. The time window size was tested from 5s to 10s, with 1s time resolution, in order to investigate time-sensitive changes in the BCI system performance. In order to determine BCI decision, the canonical correlation analysis (CCA) algorithm was employed to find the maximal correlation between EEG electrode signal and signals from a matrix of templates corresponding to the SSVEP stimulus frequencies. Based on the results of these offline experiments, online experiments were once again conducted using electrode-equipped caps. However, for online experiments, subjects were asked to spell the words "BRAIN," "CORTEX," and "MEMORY" (words widely employed in BCI spelling experiments). In order to familiarize subjects with the Bremen speller application, they carried out a short familiarization run before

online experiments commenced. In the online experiments, both visual and auditory feedback was provided in real time. The BCI decision was also carried out by CCA. Bremen BCI application with the capacitively-coupled electrode was evaluated by calculating accuracy (ACC), information transfer rate (ITR), the number of decoded letters per minute (LPM), and efficiency (EFF defined as the minimum number of commands necessary to spell the target word divided by the number of commands issued during the run [50]).

2.5.2. Auditory Steady-State Response-based BCI

The experimental paradigm described by *Kim* et. al. [51] was employed for ASSR-based BCI application. Stimuli were generated using Matlab with periodic amplitude-modulated and pure sinusoidal tones. Modulation frequencies of 37Hz and 43Hz were selected, since frequency ranges peaking around 40Hz were shown to obtain higher ASSR signal-to-noise responses [52]. In order to make auditory stimuli easily distinguishable, carrier frequencies of 2.5kHz and 1kHz were selected, respectively. Then, a 2.5kHz pure tone with 37Hz modulation frequency was presented in the left sound field (L), and a 1kHz pure tone with 43Hz modulation frequency was presented in the right sound field (R). Participants were seated on a comfortable chair approximately 60cm from a pair of commercial speakers (BR-2100S, Britz

International, Paju, Korea) while wearing a capacitively-coupled electrode installed-cap (see Figure 2-15 (b)). Electrode attachment methods were the same as previous SSVEP experiments, but positioned on the O_Z , C_Z , T_7 and T_8 sites of the normal baseball cap instead of the O_1 and O_2 sites.

In this experiment, subjects also performed offline experiments first to determine the optimal analysis window size. The participants were asked to concentrate on one of the stimuli (L or R) for 20s according to programmed auditory instructions provided immediately before the onset of each stimulus. This process was repeated 50 times; therefore, data from 25 trials for each stimulation sound were collected.

In the offline experiments, no feedback was given to subjects. For the evaluation of classification, a 10-fold cross validation method was applied. A total of 50 trials were divided into 10 folds; 45 trials were used as a training set and 5 trials were used for validation. Frequency spectrums were calculated using a nonparametric periodogram method with a 1s sliding time window and 50% overlap. The spectral density of each electrode over a stimulus frequency $\pm$1Hz range was extracted from the averaged frequency spectra and fed to a classifier as a feature vector. Classification was performed using a linear discriminant analysis (LDA) method that guarantees maximal class separation by maximizing the ratio of between-class variation to within-class variation in our dataset. Changes in the performance of the BCI system

were investigated by testing a time window size of 5s to 20s with 1s time resolution. The best result was then applied to the online experiments.

Online experiments were performed after a brief rest. During the rest time, participants briefly removed the electrode installed cap, and wore it again right before starting the online experiment. The data from the previous 50-trial offline experiments were used as a training set for the LDA application. On the basis of simple binary classification, a total of 10 trials were performed of selective attention to either left or right stimuli. Finally, the ASSR-based BCI application with capacitively-coupled electrode was evaluated according to the number of correct decisions (NUM) and information transfer rate (ITR). The specificity (SPEC) and sensitivity (SENS) were also calculated by assuming positive to be left (L) and negative to be right (R).

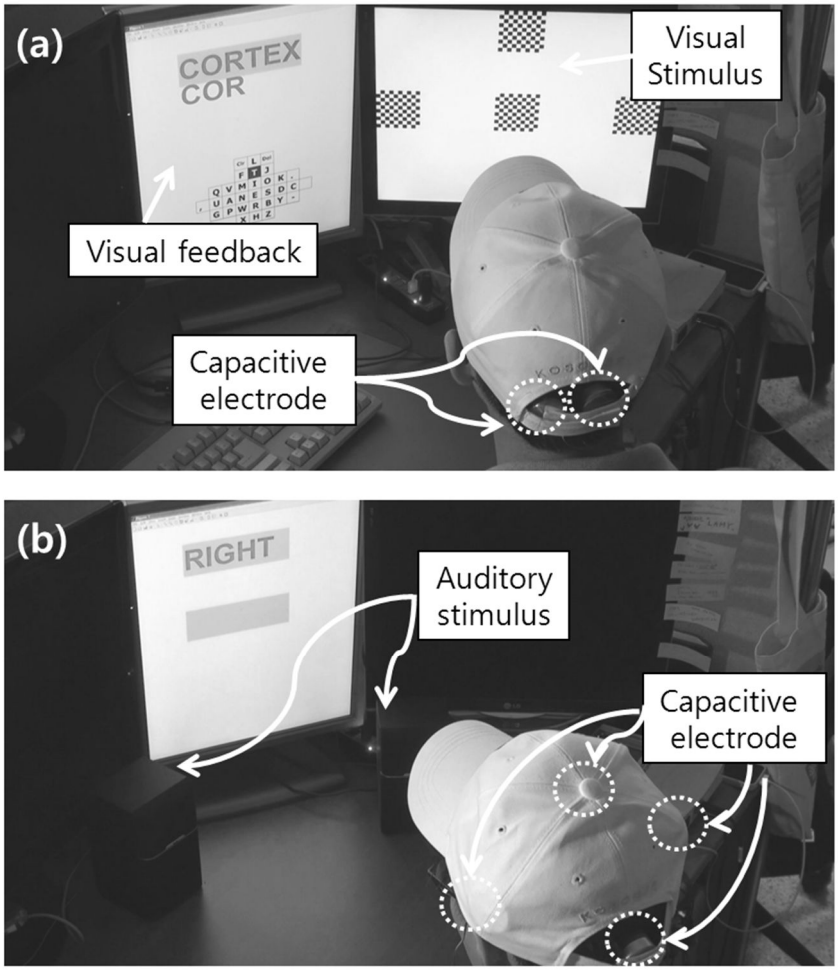

Figure 2-15. A snap shot of the experimental condition for (a) SSVEP-based BCI: The subject was trying to spell the given English word, "CORTEX", (b) ASSR-based BCI: The subject was trying to concentrate on the auditory stimulus presented in the right sound field. EEG acquisition was made while wearing a baseball cap equipped with capacitively-coupled electrodes.

3. Results

3.1. Electrode Surface-Skin Interface Impedance

Electrode-skin interface impedance varies according to various factors such as the properties of the stratum corneum, sweat glands, sweat ducts, and the applied pressure. In order to obtain reproducible measurements, electrode surface-skin interface impedance was investigated under the following conditions: 1) electrodes were placed at consistent locations with constant applied pressure; 2) all experiments were carried out in the same day; and 3) all measurements were carried out after the removal of sweat. Impedance measurements were conducted 10 times for each electrode type (Ag/AgCl, conventional rigid-surfaced capacitively-coupled and proposed foam-surfaced capacitively-coupled electrodes) according to frequency changes, and the results are shown in figure 3-1. The impedances shown are mean values with standard deviations. In figure 3-1, the diamonds denote the impedance of the proposed foam-surfaced capacitively-coupled electrode. The circles and squares denote the impedance of the Ag/AgCl and conventional rigid-surfaced capacitively-coupled electrodes, respectively. The impedances were much higher for the capacitively-coupled electrodes than for the Ag/AgCl electrode at a low frequency

range. However, lower contact impedance was always found with the foam-surfaced electrode than with the conventional rigid-surfaced electrode, especially for measurements at hairy sites [see figure 3-1 (b)]. For the biological signal frequency range, an impedance difference of about 100 kΩ for hairless sites and about 2000 kΩ for hairy sites was observed between the two kinds of capacitively-coupled electrodes. This showed that the proposed foam-surfaced electrode provided higher performance for hairy sites, evidently by showing lower impedance on the hairy sites. The conductive foam employed for this study is soft, dry, and flexible enough to contact the hairy skin properly. In other words, the soft dry foam, which will adapt to head topography, will cover a large contact area and be effective in reducing electrode-scalp interface impedance as well as enlarging coupling capacitance.

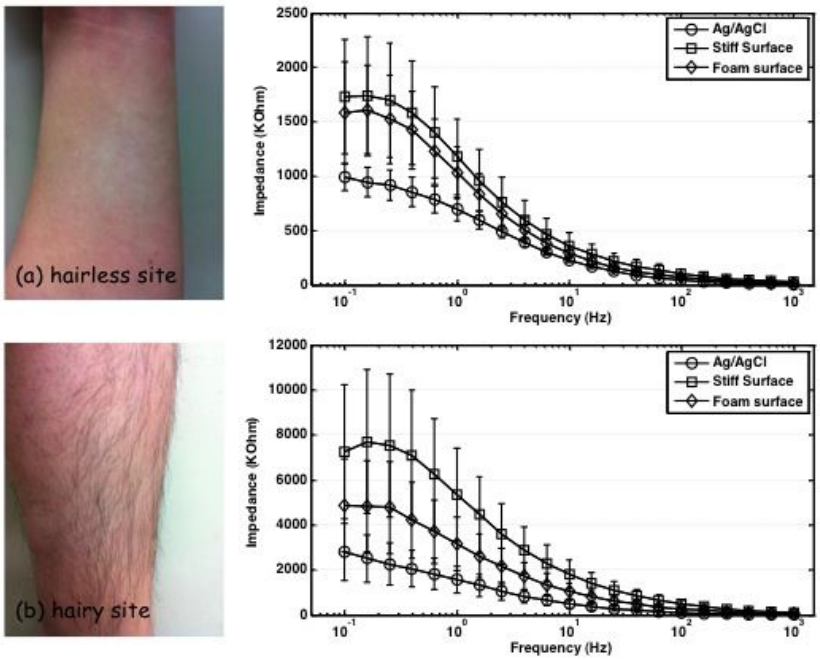

Figure 3-1. Electrode surface-skin interface impedance according to the frequency change: (a) at a hairless forearm site, (b) at a hairy ankle site.

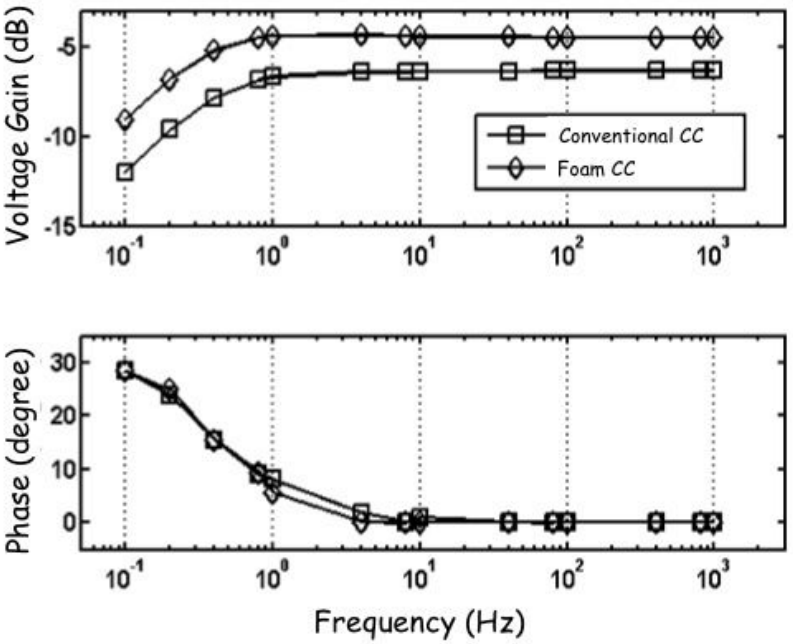

Figure 3-2. Measured gain and phase difference of the two types of capacitively-coupled electrodes though hair.

3.2. Frequency Responses of Foam-surfaced Capacitively-coupled Electrode

The frequency responses of the EEG electrodes were experimentally measured by a frequency sweep, resulting in the data shown in figure 3-2. As I expected, the frequency response shows the features of a high-pass filter, as reported in other capacitively-coupled electrode studies [33, 34, 38-42]. It showed a relatively low voltage gain and large phase difference in the low frequency range. However, the voltage gain of the proposed foam-surfaced electrode was about 2 dB higher than that of the rigid-surfaced electrode over all of experimental frequency range (0.1-1000 Hz). In addition, a stable gain response and small phase differences were obtained in the frequency range of interest (4-100 Hz) for EEG monitoring for non-clinical purposes.

3.3. Quantitative Assessment of Signal Quality

Figure 3-3 shows the results of (a) SNR and (b) SER analysis. The values in figure 3-3 represent the means and standard deviations for 10 measurement trials for each electrode type. The SNRs of the raw signals were dramatically increased from -1.34 ± 0.59 dB for the rigid-surfaced electrode to 1.88 ± 0.13 dB for the foam-surfaced electrode. The SERs were also compared and showed an overall increase (raw signal using rigid-surfaced electrode: 0.87 ± 0.14 dB; raw signal using foam-surfaced electrode: 1.39 ± 0.28 dB) when using the foam-surfaced capacitively-coupled electrode. The SNRs calculated after removing the 60-Hz power line noise were not statistically different according to electrode type; however, the mean value was higher for the foam-surfaced electrode than for the conventional rigid-surfaced electrode. The SERs calculated after the normalization of each signal showed increased values (rigid-surfaced electrode: 1.71 ± 0.41 dB; foam-surfaced electrode: 3.38 ± 0.34 dB) for the foam-surfaced electrode. In conclusion, the modification of the capacitively-coupled electrode with the soft foam surface enhanced its ability to make EEG signal measurements through hair.

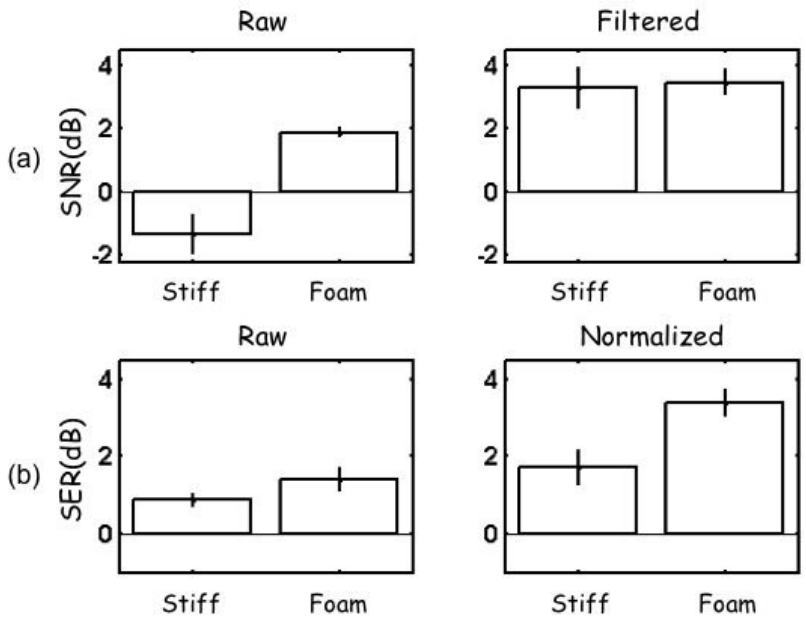

Figure 3-3. Results of (a) SNR and (b) SER analysis for conventional rigid-surfaced and proposed foam-surfaced capacitively-coupled electrodes.

3.4. EEG Measurement through Hair

Finally, the true EEG signal quality was investigated for the standard wet electrode, conventional rigid-surfaced capacitively-coupled electrode and proposed foam-surfaced capacitively-coupled electrode. Figure 3-4 shows the examples of EEG signals measured using three pairs of electrodes in the locations of (a) hairy occipital

sites (O_2) and (b) hairy parietal sites (C_4). In figure 3-4, the left y-axis indicates the scale for the capacitively-coupled electrodes and the right y-axis indicates the scale for the resistively-coupled wet electrode. Note that although the raw signal amplitudes of the wet electrode and the capacitively-coupled electrodes are not similar, their waveforms are comparable. In addition, the spectral components of the resistively-coupled and capacitively-coupled electrode signals over the frequency band of 0.05-30 Hz showed similar power spectra except for the absolute power values [Figure 3-4 (c) for O_2, (d) for C_4]. Table 3-1 shows the correlation coefficients for individual subjects. The ECG has unique shapes and features, and therefore the validation of a new recording system generally shows very high correlations. However, unlike the ECG, the EEG waveform morphology and amplitude vary significantly according to measurement locations and have no unique features like an ECG signal. Intrinsically, the EEG records signals originating from many synapses in a few cortical regions, so EEG recordings are considered to be a mixture of signals from spatially broad areas. Although measurements were performed at neighboring sites using three kinds of electrodes in this study, their exact positions differed. In addition, the relatively large areas of capacitively-coupled electrodes caused a spatial averaging effect of regions of no interest on the measured signals. Considering these measurement conditions, the resulting correlation coefficients were acceptable

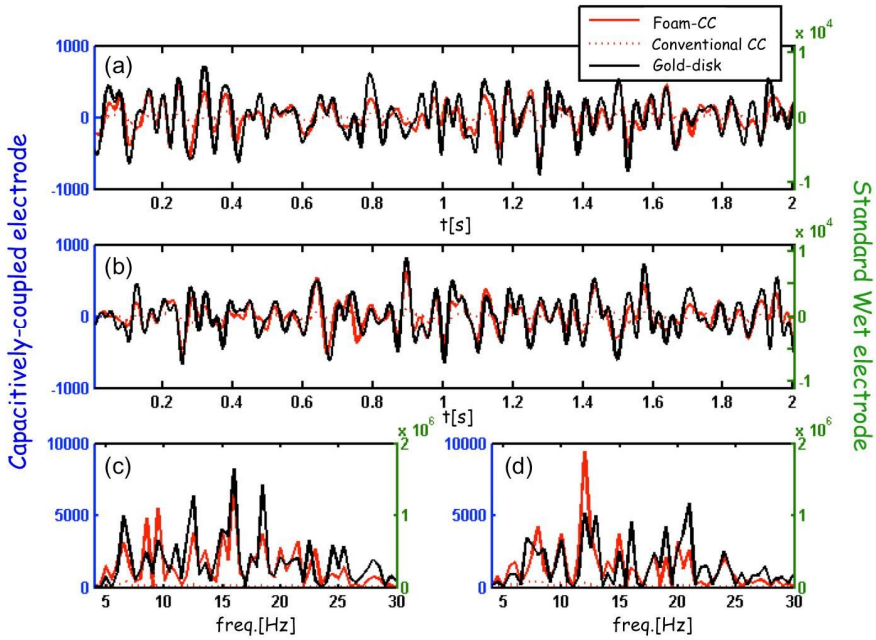

Figure 3-4. Comparisons of EEG signals measured by standard wet, conventional capacitively-coupled and proposed foam-surfaced capacitively-coupled electrodes. (a) EEG at occipital location, (b) EEG at parietal location, (c) power spectrum of (a), (d) power spectrum of (b).

for the validation of the newly presented electrodes. (Averaged correlation coefficient between EEGs measured at same locations, but using two standard wet electrodes over five subjects was 0.793 ± 0.08 for occipital site and 0.858± 0.10 for parietal site, respectively). The EEG signals shown in figure 3-4 suggest that the capacitively-coupled EEG measurements conformed to the EEG measurement from the standard wet electrode.

It is concluded that the EEG signals recorded by paste-based and capacitively-coupled electrodes were similar, and although capacitively measured EEG through hair may not be acceptable for clinical situations and medical applications, they are sufficient for non-medical purposes in out-of-hospital applications. A simple alpha wave experiment was employed as a basic validation of the proposed foam-surfaced capacitively-coupled electrode for BCIs and out-of-hospital monitoring applications. For this experiment, a foam-surfaced capacitively-coupled electrode was attached to a regular baseball cap worn by the subject.

Figure 3-5 shows an example of the baseball cap used for nonintrusive wearable capacitively-coupled EEG measurement. The rigid-surfaced electrode was attached to the O_1 site and the foam-surfaced electrode was attached to the O_2 site of the baseball cap for comparison; these electrodes did not contact the bare scalp. Figure 3-6 shows an EEG signal taken during a trial where a subject was asked to open and close their eyes during the segment spanning 5-20 s into the trial. In this case, a clear alpha wave was successfully acquired during the closed eye period with both electrodes; however, the EEG signals from the foam-surfaced electrode [Figure 3-6 (b)] were four times larger than those of the rigid-surfaced electrode [Figure 3-6 (a)].

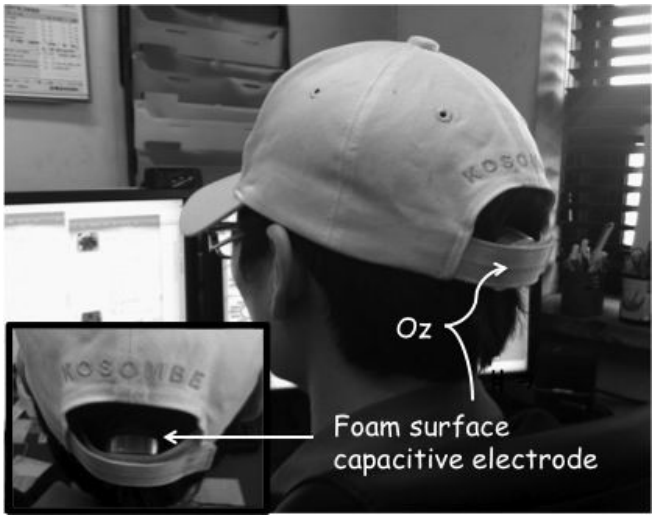

Figure 3-5. The subject wore a conventional baseball cap in which the proposed foam-surfaced capacitively-coupled electrode was installed at site O_z.

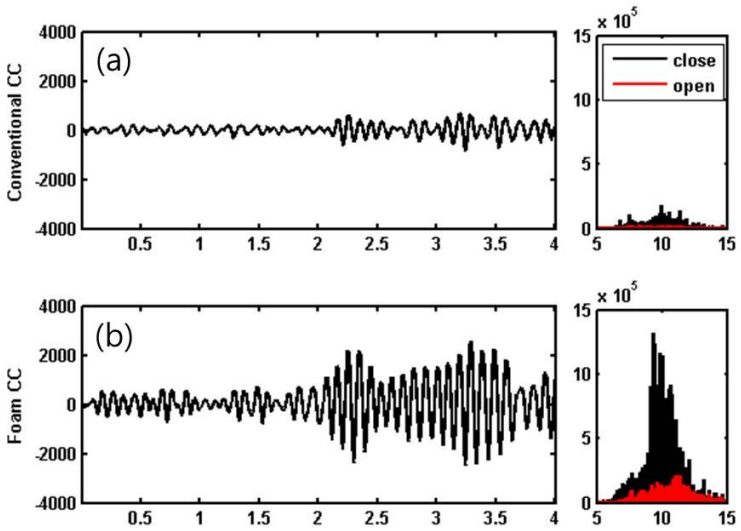

Figure 3-6. Capacitively-coupled measurement of the EEG alpha wave and its spectra: alpha frequency range was enhanced during the closed-eye section.

Table 3-1. Correlation coefficients between EEGs measured by a standard wet electrode and a capacitively-coupled electrode at an occipital site O_2 and a parietal site C_4.

	O_2		C_4	
	R-CC[a]	F-CC[b]	R-CC[a]	F-CC[b]
S1	0.575	0.855	0.535	0.848
S2	0.578	0.789	0.649	0.779
S3	0.547	0.852	0.539	0.746
S4	0.701	0.784	0.685	0.771
S5	0.095	0.586	0.369	0.789
Mean	0.499	0.773	0.555	0.787
± SD	± 0.12	± 0.05	± 0.06	± 0.02

[a]R-CC: Rigid-surfaced capacitive electrode.
[b]F-CC: Foam-surfaced capacitive electrode.

3.5. SSVEP using Capacitively-coupled Measurement

Figure 3-7 shows the classification accuracies and ITR for each participant with respect to different analysis window sizes. When the CCA algorithm was applied, the averaged classification accuracy for all subjects was 85.6, 88.0, 95.2, and 97.6% for window sizes 4, 5, 6 and 10s, respectively. Although the 10s time window showed excellent performance, there are trade-offs between time window size and accuracy as well as other BCI variable performances such as ITR and LPM. Considering this point, an analysis window size of 6s was selected as optimal for all participants in this study. Although shorter time periods, about 4s, are generally employed for SSVEP-BCI when a conventional Ag/AgCl electrode is used, this increased time

window is required for capacitively measured EEG because of reduced signal-to-noise ratio. The time window of 6s is also recommended by *Chi et al.,* who performed capacitively-coupled SSVEP-based phone dialing task using this time window [53]. Based on these offline experimental results, online experiments were performed using a 6s analysis time window.

Table 3-2 presents the online experimental results for each participant. The average accuracy, ITR, LPM, and EFF were 91.21%, 17.78 bits/min, 3.41 letters/min, and 82.42%, respectively. Of note, since the classification accuracy of subject 3 (S3) was 100% for all copy and spelling tasks using an analysis time window of 6s, the subjects performed additional online experiments for analysis time windows of 4s and 5s. In this case, the results for 4s included averaged ACC 79.21%, ITR 13.27 bits/min, LPM 3.36 letters/min, and EFF of 58.43%. Results for 5s were averaged ACC 93.5%, ITR 21.31 bits/min, LPM 4.01 letters/min, and EFF 86.98%. Our results were comparable to previously reported findings in literature using the Bremen BCI system with conventional Ag/AgCl electrodes. Considering the presented experimental results, It was able to confirm that the polymer foam-based capacitively-coupled EEG electrode could be used for various SSVEP-based BCI applications. A demonstration video can be found on website at http://baek.re.kr as well as http://www.youtube.com/watch?v=eFktIckFqac.

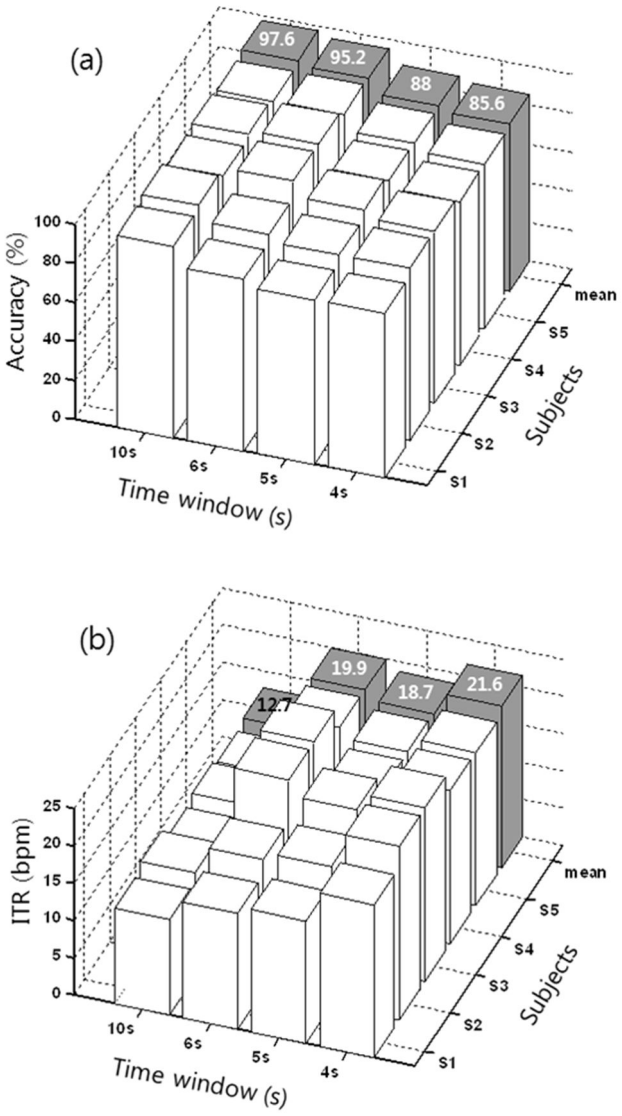

Figure 3-7. Offline SSVEP analysis: (a) classification accuracy, (b) ITR for each participant with respect to different analysis time window sizes.

Table 3-2. The results of SSVEP-based online BCI experiments. (ACC: accuracy in %, ITR: information transfer rate in bit min^{-1}, LPM: letters per minute in letter min^{-1} and EFF: efficiency in %)

Word	Sub.	Time Window	Input results (wrong underlined)	ACC (%)	ITR (bits/ min)	LPM (letters/ min)	EFF (%)
BRAIN	S1	6s	→↓B↓R←←A↑I↑←↓N	92.86	16.79	3.57	85.71
	S2	6s	↓→B↓R←←A↑I←N	100	23.22	4.17	100
	S3	4s	↓↑↓→B↑↓↓R←←A↑I←←→N	83.33	14.50	4.17	66.67
		5s	↓→B↓R←←A↑I←N	100	27.86	5	100
		6s	↓→B↓R←←A↑I←N	100	23.22	4.17	100
	S4	6s	↓→→→←←B↓R←←A↑I←N	87.5	15.67	3.13	75
	S5	6s	→↓B↓R←←←→A↑I←N	92.86	16.79	3.57	85.71
CORTEX	S1	6s	→→→C↓→↑↑O↓R↑↑TE↓↓←↑↓X	90.48	15.18	2.98	80.95
	S2	6s	→→→→←C↑→O↓R↑↑TE↓↓←X	94.74	18.18	3.16	89.47
	S3	4s	↓↑→→→→←C→→←↑O←←→→↓R↑↑TE↓↓↑↓←X	79.31	13.95	3.10	58.62
		5s	→→→C←↑→→O↓R↑↑T←→E↓↓←X	90.48	18.22	3.43	80.95
		6s	→→→C↑→O↓R↑↑TE↓↓←X	100	23.22	3.53	100
	S4	6s	→→→C↑→O←→↓R↑↑TE↓↓←X	94.74	18.18	3.16	89.47
	S5	6s	→→→C→↑O↓↓↑R↑↓↑↑TE↓→←↓←X	86.96	13.07	2.61	73.91
MEMORY	S1	6s	←↑ME←↓↑↑M→↑O↓R→→↓Y	94.44	17.95	3.33	88.89
	S2	6s	↑←ME↑←M↑→O↓↓↑R↓→→→←Y	90	14.88	3	80
	S3	4s	↑←ME↑←←→→←M↑←→→O↑↓↓→←R↓↓←→→←↑→→Y	75	11.37	2.81	50
		5s	↑←M↑↓E↑←M↑→O↓R↓→→→←Y	90	17.85	3.6	80
		6s	↑←ME↑←M↑→O↓R↓→→Y	100	23.22	3.75	100
	S4	6s	←↑ME←←→↑M→↑↑↑↓↓O↓R→→↓Y	86.36	15.01	2.73	72.73
	S5	6s	←↑ME←↑M←→→↑O↓→←R→→→↓←Y	86.36	15.01	2.73	72.73
Mean				91.21	17.78	3.41	82.42

3.6. ASSR using Capacitively-coupled Measurement

The classification accuracy and individual ITR with respect to time window sizes are presented in Figure 3-8. The maximum classification accuracy of each participant ranged from 81.7 to 91.7%, depending on the different size of the analysis time window. Overall, classification accuracy increased with increased analysis time window size. The bold line in Figure 3-8 indicates the average accuracy and ITR for all subjects. Average classification accuracy increased in a linear fashion with respect to window size, but no longer increased after about 14s. This relationship was also seen by *Kim et al.* in a study using conventional wet electrodes but shorter time lengths (10s) compared to our results of 14s [51].

Similar to the SSVEP responses, capacitively-coupled measurement of ASSR also required more time for sufficient rejection of the extra noise. Ultimately, a 14s analysis time window was employed for online experiments. Table 3-3 presents the online experimental results for each participant. The results were as follows: average NUM 7.2/10, SPEC 0.64, SENS 0.76, and ITR 0.7 bits/min. The recently proposed ASSR-based auditory BCI technique is a relatively new concept, which is the subject of ongoing research in vision-free BCI systems [51]. In comparison to results from other BCI paradigms such as SSVEP, this study's results are not strong enough yet to

support direct application of BCI. However, the results obtained in this study are comparable to previously reported results from the same ASSR-based paradigm using conventional Ag/AgCl electrodes (online classification accuracy of 14 continuous trials: 71.4%). Considering our experimental results, future research could continue to investigate the use of our polymer foam-based capacitively-coupled EEG electrode in ASSR-based BCI applications. A video demonstrating the use of capacitively-coupled electrode for ASSR-BCI also can be found on our website at http://baek.re.kr as well as http://www.youtube.com/watch?v=emKvgvKaHuw.

Table 3-3. The results of ASSR-based online BCI experiments. (NUM: number of correct classification per total number of trials, SEPC: specificity, SENS: sensitivity and ITR: information transfer rate in bit min^{-1}). The wrong classification is underlined.

Sub.	Time window	Task	Classification Results	NUM (correct/total)	SPEC	SENS	ITR (bits/min)
S1	14s	LLRRLRLRLR	LLLRLRRLRR	6/10	0.6	0.6	0.12
S2	14s	RRRLRLLLRL	LRRLLLLLLL	7/10	0.4	1	0.51
S3	14s	LRRLLRLRLR	LRLLLRRRLR	8/10	0.8	0.8	1.19
S4	14s	LLRRLRLLRR	LRRRLRRLRL	7/10	0.8	0.6	0.51
S5	14s	LLRRLRLRLR	LLRLLRRRLR	8/10	0.6	0.8	1.19
	Mean			7.2/10	0.64	0.76	0.70

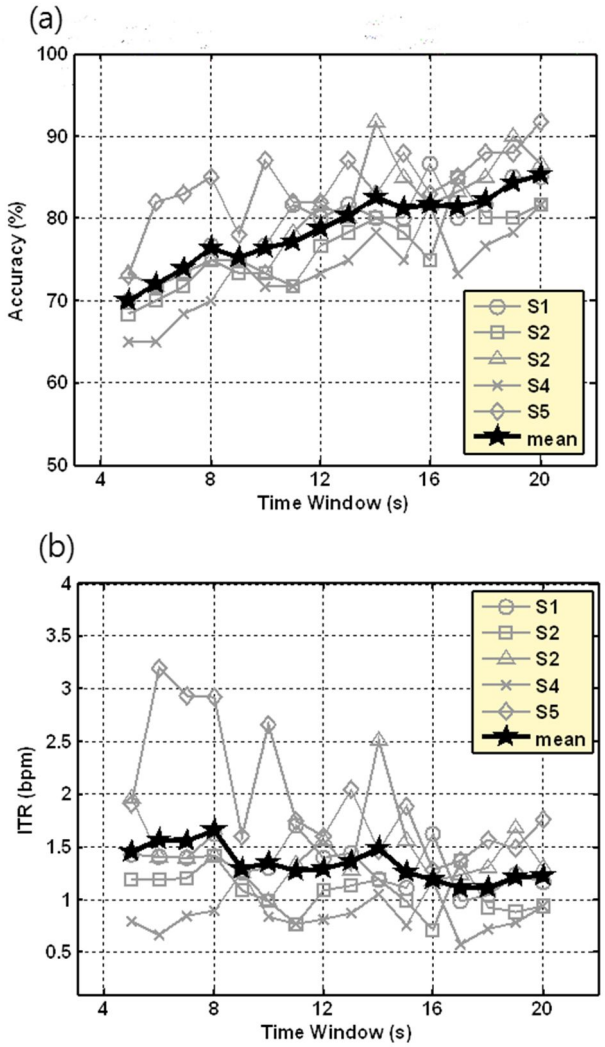

Figure 3-8. Offline ASSR analysis: (a) classification accuracy, (b) ITR for each participant with respect to different analysis time window sizes.

4. Discussion

4.1. The Foam-surfaced Capacitively-coupled Electrode

In this study, a capacitively-coupled EEG electrode incorporating a polymer foam surface was proposed and evaluated as a nonintrusive and convenient monitoring method for out-of-hospital EEG measurements. While most EEG monitoring uses dry contact electrodes that require some scalp/hair preparation procedures in order to make contact between the electrodes and bare scalp, in the present study, I investigated the feasibility of EEG measurement without any electrical contact through hair using dry electrodes. Using same capacitively-coupled biopotential measurement method applied in previous studies [39, 40, 54], the modification of electrode surface was found absolutely to enhance its performance. In capacitively-coupled EEG measurement, coupling capacitance is defined as $C = (\varepsilon_0 \varepsilon_r A)/d$, where A is the area of the electrode surface, d is the distance between the scalp and electrode surface, ε_0 is vacuum permittivity and ε_r is the dielectric constant of the hair. For capacitively-coupled electrodes, the capacitor plate is defined by the electrode surface and scalp skin, an inhomogeneous layer.

Profer definition of the capacitor is difficult, as the definition depends on the skin

structure and the amount of sweat secretion, which changes over time. The dielectric constant is not only defined by the insulating layer, but also by gaps between the scalp skin and the electrode surface. Conventional rigid-surfaced capacitively-coupled electrodes produced an undefined contact area due to their rigidity and locally isolated hairs between the electrode surface and scalp skin. This affected the contacting area and dielectric constant as well as distance, resulting in a low SNR signal, which made signal measurement impossible. In contrast, the foam material employed in this study adapts to scalp topography such as curvature and hair, and experiences low relative motion of the scalp to the electrode because of its flexibility and cushioning effect. The foam-surfaced capacitively-coupled electrode provided lower skin-electrode interface impedance than the conventional rigid-surfaced one under the same measurement conditions, especially for the hairy measurement sites. This can be explained by the fact that the softness of the foam electrode substrate can help to adapt to the skin effectively when suitable force is applied, since it is clear that contact area and skin-electrode impedance are negatively correlated: large number of air gaps between the rigid electrode surface and hair will decrease the effective contact area and significantly increase electrode-skin interface impedance.

Enhanced performance due to the foam surface in the proposed capacitively-coupled electrode was also revealed in frequency response experiments. For all of the

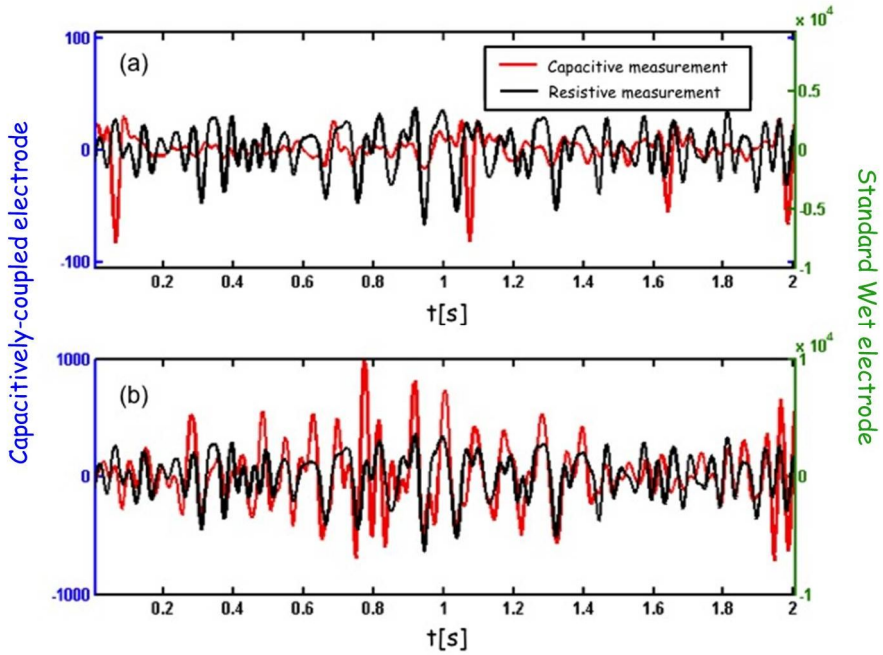

Figure 4-1. Capacitively-coupled measurement of the EEG at O_2 for subject 5: EEG measurement failed with the conventional rigid-surfaced capacitively-coupled electrode (a) while the proposed foam-surfaced capacitively-coupled electrode successfully measured EEG (b).

frequency ranges tested in this study, the foam-surfaced electrode showed a much higher voltage gain and slightly lower phase difference compared to the reference signal than the rigid-surfaced electrode. The foam-surfaced electrode was also associated with higher SNR and SER values than the rigid-surfaced electrode. The correlation coefficients between the reference signal and capacitively measured signals also showed enhanced performance with the employment of the foam surface for all tested frequency ranges. In addition, the foam-surfaced capacitively-coupled

electrode is expected to provide not only significantly higher SNR and SER—, but also better stability of the skin-electrode interface impedance for long-term use,—because it does not require a conduction gel or paste that is prone to drying out. Finally, direct comparisons between capacitively measured EEGs and those measured using wet electrodes showed that the correlation coefficients were dramatically improved for both O_z and C_z sites when employing a foam-surfaced capacitively-coupled electrode. For subject 5, EEG measurement at the O_2 site was impossible with the conventional rigid-surfaced electrode, while the foam-surfaced electrode successfully measured an EEG signal (see figure 4-1).

In conclusion, the signal quality achieved using our foam-surfaced capacitively-coupled electrode is not identical to the standard wet electrode, but is comparable, while the conventional rigid-surfaced electrode did not perform as well. Based on this study, our results showed that the proposed foam-surfaced capacitively-coupled electrode presents a different but effective alternative to acquiring EEG signals without wet electrodes for non-clinical purposes in out-of-hospital environments. It should be possible to record EEG signal measurements while simply wearing a cap or helmet with proposed foam-surfaced electrodes installed in appropriate montages without the need to remove scalp hair.

The proposed addition of the foam surface to a conventional capacitively-coupled

electrode improved its performance in EEG measurement; however, it also has limitations. First, a study on reducing the electrode size should be performed. This will be difficult, since coupling capacitance is proportional to electrode size. The diameter of the capacitively-coupled electrode employed in the current study was 36 mm, much larger than conventional EEG electrodes (typically 5-10 mm). This may lead to severe spatial averaging of individual neuronal signals as compared with conventional EEG electrodes. In addition, due to the size constraint, high-density EEG monitoring may not be possible. Although it seems to be sufficient for use in general purpose low-density EEG monitoring, the minimization of the capacitively-coupled electrode may be required for clinically valuable information acquisition.

I observed that the absence of adhesive materials in dry EEG electrodes resulted in poor contact between the electrode and head surface. Therefore, for nonintrusive wearable EEG applications, ensuring the appropriate contact of electrodes to the head when they have been mounted on a cap is also a critical problem to be solved for successful capacitively-coupled EEG measurement. In the present study, foam-surfaced capacitively-coupled electrodes were attached to a regular baseball cap without any additional structures for adapting electrodes to the head, and therefore there was not enough pressure to create optimal contact, especially for the parietal EEG, which may have produced signal noise. In future studies, electrodes should be

flexibly mounted using spring-like structures to ensure sufficient applied pressure.

Movement artifacts also need to be removed. In this study, all experiments were performed while the subject sat in a comfortable chair without bulk movements. Since detection of a movement-free period may be enough for the application of the proposed method for monitoring purposes such as healthcare, any movement artifact removal or compensation methods was not applied in the current version. The minimization of motion artifacts in capacitively-coupled biopotential measurements has been addressed through several studies [55-57]. Consequently, capacitively-coupled EEG during movement can be properly measured on the proposed foam-surfaced electrode using various techniques and methods for the future wearable EEG measurement applications. Finally, it is necessary to conduct the method on a wider population including groups with different ages, genders, and neurological disease status.

Recently, the amount of attention paid to EEG monitoring during usual daily life has increased. The most often represented example is BCIs ranging from assistive technologies for people with severe motor disabilities to entertainment for healthy people. Most studies regarding BCIs have focused on signal processing or its application methods for enhancing information transfer rate and accuracy or to increase the number of classifications. So far, issues regarding brain signal sensing

methods such as portability, comfort, ease of use or aesthetic sensor design have not been required in BCI research. In order to translate laboratory experiments into real world applications in out-of-hospital or laboratory environments, these issues should be addressed.

In the current study, I implemented an EEG system using a regular baseball cap that used dry electrodes to record EEG signals regardless of the presence of hair. This system should be considered for real world applications of EEG devices in out-of-hospital environments, and the proposed foam-surfaced capacitively-coupled electrode met the requirements of such systems. I am currently investigating foam-surfaced capacitively-coupled electrode applications for BCI technologies with wide range of paradigms including SSVEP, ASSR, P300, and motor imagery and it is expected that at least, steady-state visual evoked potential-based BCI that has been previously reported using conventional rigid electrodes will be much more effective using the proposed foam-surfaced electrode [53, 58].

4.2. BCI using Capacitively-measured EEG

The brain-computer interface (BCI) is at the forefront of current neural engineering research. Thus far, progress in BCI mainly has been made in enhancing BCI performance. As a result, most of the BCI literature focuses on advanced signal processing methods or new innovative paradigms. However, in order to improve the use of BCI among various different user groups and to enhance its real-world application, BCI flexibility, accessibility, and usability must be improved. In 2012, *Liao et al.* proposed the concept of augmented BCI (ABCI) that can be used by individuals for everyday use [59]. By employing advanced biosensing techniques, including dry electrodes, ABCI aims to expand the application of BCI technologies from the current laboratory or clinical settings to normal daily life.

As described before, various dry contact EEG electrodes have been developed. These electrodes have comparable performance and EEG measurement compared to standard wet electrode. However, they do not meet the ideal goals of ABCI. MEMS/carbon nanotube-based electrodes are slightly invasive. Fabric-based electrodes have difficulty measuring EEG signals at sites covered with hair. Hybrid-type or spring-loaded electrode finger-based EEG sensors allow for EEG acquisition at hairy sites, but require preparation in order to ensure contact between finger and

scalp. These limitations make it difficult to integrate sensing devices into accessories such as baseball caps, headbands, or helmets that could be used for natural state EEG monitoring.

Capacitively-coupled electrodes that do not require any electrical contact between sensor and scalp are promising tools for the future of ABCI. However, developing capacitively-coupled EEG electrodes still remains a challenge, given the need for improvements in EEG sensing despite high source impedance, head curvature, and undefined contact area due to hair. This study introduced a new capacitively-coupled EEG electrode that employs a conductive polymer foam surface that attempts to overcome the aforementioned problems. Of note, it is the first to investigate implementation of polymer foam-based capacitively-coupled EEG electrode for BCI applications.

In SSVEP experiments, the average classification accuracy was comparable to previous studies using the Bremen BCI paradigm with conventional wet electrode. However, average ITR was lower (17.78 bpm) compared to previous studies (26.56 bpm [48] and 22.60 bpm [49]). ITR depended on accuracy, selection number, and speed. In our experiment, decisions were made at every fixed time window without overlapping window sliding. This allowed for convenience in the experimental setting. It is expected that ITR would have increased if a sliding-window decision

method to reduce decision time was employed.

Previous studies recorded EEG data from more than five electrodes at the parietal and occipital cortex. However, data were measured from only the O_1 and O_2 sites in this study. Moreover, previous studies utilizing the Bremen BCI paradigm with wet electrodes used a full Bremen BCI system for all aspects of the SSVEP display, real-time signal processing, feedback, and storage. The online signal processing included more complex methods than the CCA that was used in this study. ASSR-based BCI paradigm employed was first introduced in 2011 by *Kim et al* [51]. In their experiments (n=6), offline analysis showed that classification accuracy increased linearly with respect to analysis window size, but no longer increased after approximately 10s. The average maximum classification accuracy of each participant was about 86.33±3.54%, and the analysis window size that resulted in the highest accuracy was 14±2.94s. In the current study (n=5) using capacitively-coupled electrodes, I was also able to find that classification accuracy was increased with respect to analysis time window size, but only until 14s. This relationship was also seen in other capacitively-coupled SSVEP experiments. *Chi et al.* found that compared to wet electrodes, increased analysis time window is required for capacitively-coupled SSVEP measurement for sufficient rejection of the extra noise seen in capacitively-coupled measurements [53]. The average analysis time window

size for highest accuracy was larger than Kim's result (17±1.33s). The average maximum accuracy for each participant was slightly lower than Kim's results (85.84±2.46%) but exceeded the chance level of binary classification (50%). Additionally, the maximum ITR in online experiments had a minimal difference of 0.01bpm between studies (1.2bpm for Kim's study vs. 1.19bpm for our study) [51].

Finally, the presented experiments were carried out in a normal office environment and the ambient light, noise and electrical devices were left turned on throughout the day. This environment was significantly different from that of other studies, which were performed in an electrically shielded, dimly lit, or sound proofed rooms. Considering these experimental conditions, experimental results demonstrated the potential for using capacitively-coupled EEG electrode as alternative to conventional wet electrode in everyday ABCI applications.

To my knowledge, only two publications have addressed BCI with capacitively-coupled EEG electrodes [53, 58]. *Oehler et al.* first reported capacitively-coupled EEG application for SSVEP-based BCI in 2008 [58]. Active electrodes were constructed using a standard PCB plate. Unlike the current electrode, the sensing plate was rigid and did not have a cushioning effect. They tested three-channel capacitively-coupled EEGs at the occipital region and performed three-class classifications. Although they did not provide individual results for online

experiments, they reported a maximum accuracy of 95% and a maximum ITR of 12.5bpm. In 2012, *Chi et al.* also performed capacitively-coupled EEG application for SSVEP-based BCI [53]. Their electrodes also had a rigid sensing surface, but they constructed a full custom sensor front-end that improved input impedance of the active electrode. In their experiments, two subjects performed a 12-digit phone dialog task with an average accuracy of 83% and ITR of 14.5bpm.

Although the signal processing methods and BCI application tasks were different, this paper reports the best performance for capacitively-coupled SSVEP-based BCI. Moreover, the present work is the first study on a capacitively-coupled EEG application for ASSR-based BCI to have testable results comparable to those performed using conventional wet electrodes.

In this study, a newly developed capacitively-coupled electrode was effective in steady-state response based BCI paradigms. However, further studies are needed to better develop this technique. BCI experiments were conducted using only steady-state responses since they are well-defined and repeatable. Further experiments using the proposed electrode should be applied to different BCI paradigms using event-related potentials (ERP) including P300, visual evoked potentials, or auditory evoked potentials.

The most critical drawback of the current capacitively-coupled electrode is its

motion artifact. This may make capacitively-coupled electrode application for ERP difficult since its waveforms consist of a series of positive and negative deflections. Movement artifact easily obscures the signal of interest, leading to serious distortions of an average ERP waveform. Therefore, further studies are needed to evaluate the proposed electrode for ERP-based BCI systems and to develop solutions to these technical problems. The measurement techniques used in present study also need further improvement for realization of the goals of ABCI. The EEG signals were collected using wires, which is inconvenient for subjects trying to live their ordinary lives. Wireless telemetry EEG systems should be considered to develop a practical, more wearable, device. Readout integrated circuits, including EEG amplifier and ADC, should be minimized in size and lightened in order to construct a wearable device. Finally, new innovative BCI paradigms that do not lead to fatigue due to direct visual or auditory stimulation should be studied and combined with the present capacitively-coupled electrode in order to design a truly user-friendly ABCI.

5. Conclusion

Recent significant progress in dry EEG electrodes has enabled many applications for out-of-hospital EEG monitoring in the areas of healthcare and BCI. Unlike most other dry electrodes, foam-surfaced capacitively-coupled electrode produced an EEG signal detected through the hair that compared well with the one recorded with a standard wet electrode. In addition, its performance was better than that of the conventional rigid-surfaced capacitively-coupled electrode. The proposed electrode will provide better comfort to users than other methods such as wet electrodes or other dry electrodes, and thus can be used for long term and daily use in EEG applications. In summary, I believe that the new EEG electrode moves the state of the art closer towards one of the future desired EEG systems, because it is: (1) easy to use, requiring minimum time to install and remove (just wearing an EEG cap in which the proposed electrodes are installed); (2) portable, so people can use it at home and during daily activities; and (3) aesthetic, so that application EEG measuring devices in out-of-hospital environments does not make users look strange.

In the present study, I also investigated whether a newly developed polymer foam-based capacitively-coupled electrode can be used in steady-state response-based BCI applications. Using the proposed capacitively-coupled electrode, EEG was

successfully measured without direct scalp contact in subjects wearing electrode-equipped baseball caps. Experimental results demonstrated that BCI performance was comparable to those reported using conventional wet electrodes. I conclude that the proposed electrode provides a more flexible and non-intrusive tool that should be further studied in the next generation of BCI technology.

Bibliography

[1] A. Kübler, F. Nijboer, J. Mellinger, T. M. Vaughan, H. Pawelzik, G. Schalk, D. J. McFarland, N. Birbaumer, and J. R. Wolpaw, "Patients with ALS can use sensorimotor rhythms to operate a brain-computer interface," *Neurology,* vol. 64, pp. 1775-7, May 24 2005.

[2] E. W. Sellers and E. Donchin, "A P300-based brain-computer interface: initial tests by ALS patients," *Clin Neurophysiol,* vol. 117, pp. 538-48, Mar 2006.

[3] H. J. Baek, H. B. Lee, J. S. Kim, J. M. Choi, K. K. Kim, and K. S. Park, "Nonintrusive biosignal monitoring in a car to evaluate a driver's stress and health state," *Telemed J E Health*, vol. 15, pp.182-189, Mar, 2009.

[4] K. K. Ang, C. Guan, K. S. Chua, B. T. Ang, C. W. Kuah, C. Wang, K. S. Phua, Z. Y. Chin, and H. Zhang, "A large clinical study on the ability of stroke patients to use an EEG-based motor imagery brain-computer interface," *Clin EEG Neurosci*, vol. 42, pp. 253-8, Oct 2011.

[5] J. Seo, J. Choi, B. Choi, D. U. Jeong, and K. Park, "The development of a nonintrusive home-based physiologic signal measurement system," *Telemed J E Health*, vol. 11, pp. 487-95, Aug 2005.

[6] R. Song, K. Y. Tong, X. Hu, and L. Li, "Assistive control system using continuous myoelectric signal in robot-aided arm training for patients after stroke," *IEEE Trans Neural Syst Rehabil Eng*, vol. 16, pp. 371-9, Aug 2008.

[7] S. Skoczen, J. Gozdzik, A. Krasowska-Kwiecien, O. Wiecha, W. Czogala, A. Wedrychowicz, and D. Zygadlo, "Can brain-machine interface improve quality of life of patients with chronic motor dysfunction?," *Przegl Lek*, vol. 67, pp. 80-2, 2010.

[8] E. W. Sellers, "Clinical applications of brain-computer interface technology," *Clin EEG Neurosci*, vol. 42, pp. IV-V, Oct 2011.

[9] J. N. Mak and J. R. Wolpaw, "Clinical Applications of Brain-Computer Interfaces: Current State and Future Prospects," *IEEE Rev Biomed Eng*, vol. 2, pp. 187-199, 2009.

[10] J. R. Wolpaw, N. Birbaumer, D. J. McFarland, G. Pfurtscheller and T. M. Vaughan, "Brain-computerinterfaces for communication and control," *Clin Neurophysiol*, vol. 113, pp.767-91, 2002.

[11] F. Nijboer et al, "A P300-based brain-computer interface for people with amyotrophic lateralsclerosis," *Clin Neurophysiol*, vol. 119, pp. 1906-16, 2008.

[12] A. Kübler, A. Furdea, S. Halder, E. M. Hammer, F. Nijboer and B. Kotchoubey, "A brain–computer interface controlled auditory event-related potential (P300) spelling system for locked-in patients," *Ann N Y Acad Sci*, vol. 1157, pp. 90-100, 2009.

[13] K. Shindo, K. Kawashima, J. Ushiba, N. Ota, M. Ito, T. Ota, A. Kimura and M. Liu, "Effects of neurofeedback training with an electroencephalogram-based brain–computer interface for hand paralysis in patients with chronic stroke: a preliminary case series study," *J Rehabil Med*, vol. 43 pp. 951–957, 2011.

[14] L. D. Liao, C. Y. Chen, I. J. Wang, S. F. Chen, S. Y. Li, C. W. Chen, J. Y. Chang and C. T. Lin, "Gaming control using a wearable and wireless EEG-based brain-computer interface device with novel dry foam-based sensors," *J Neuroeng Rehabil*, vol. 9:5, 2012.

[15] G. Schalk, D. J. McFarland, T. Hinterberger, N. Birbaumer and J. R. Wolpaw, "BCI2000: A general-purpose brain-computer interface (BCI) system," *IEEE Trans Biomed Eng*, vol. 51 pp. 1034-43, 2004.

[16] H. J. Hwang, J. H. Lim, Y. J. Jung, H. Choi, S. W. Lee and C. H. Im, "Development of an SSVEP-based BCI spelling system adopting a QWERTY-style LED keyboard," *J Neurosci Methods*, vol. 208, pp.59-65, 2012.

[17] J. Höhne, K. Krenzlin, S. Dähne and M. Tangermann, "Natural stimuli improve auditory BCIs with respect to ergonomics and performance," *J Neural Eng*, vol. 9 045003, 2012

[18] N. Ishikawa, Y. Kobayashi, M. Kobayashi, "A case of frontal lobe epilepsy in which amplitude-integrated EEG combined with conventional EEG was useful for evaluating clusters of seizures," *Epilepsy Behav*, Vol. 8, pp. 485-487, 2010.

[19] P. Kaplan, A. O. Rossetti, "EEG patterns and imaging correlations in encephalopathy: encephalopathy part II," *J Clln Neurophysiol*, Vol. 28, pp. 233-251, 2011.

[20] E. F. M. Wijdicks, P. N. Varelas, G. S. Gronseth, D. M. Greer, "Evidence-based guideline update: determining brain death in adults," *Neurology*, vol. 74, pp. 1911-1918, 2010.

[21] M. Teplan, "Fundamentals of EEG measurement," *Measurement science review*, vol. 2, pp. 1-11, 2002.

[22] A. Searle and L. Kirkup, "A direct comparison of wet, dry and insulating bioelectric recording electrodes," *Physiol Meas*, vol. 21, pp. 271-283, May 2000.

[23] R. P. Patterson, "The electrical characteristics of some commercial ECG electrodes," *J Electrocardiology*, vol. 11, pp. 23-26, 1978.

[24] Y. G. Lim, K. H. Hong, K. K. Kim, J. H. Shin, S. M. Lee, G. S. Chung, H. J. Baek, D. U. Jeong and K. S. Park, "Monitoring physiological signals using nonintrusive sensors installed in daily life equipment," *Biomed Eng Lett*, vol. 1, pp. 11-20, 2011.

[25] M. S. Fernandes, K. S. Lee, R. J. Ram, J. H. Correia and P. M. Mendes, "Flexible PDMS-based dry electrodes for electro-optic acquisition of ECG signals in wearable devices," in *Conf Proc IEEE Eng Med Biol Soc*, pp. 3503-3506, 2010.

[26] J. Yoo, L. Yan, S. Lee, H. Kim and H. J. Yoo, "A wearable ECG acquisition system with compact planar-fashionable circuit board-based shirt," *IEEE Trans Inf Technol Biomed*, vol. 13, pp. 897-902, 2009.

[27] J.-C. Chiou, L.-W. Ko, C.-T. Lin, C.-T. Hong, T.-P. Jung, S.-F. Liang, and J.-L. Jeng, "Using novel MEMS EEG sensors in detecting drowsiness application," in *IEEE Biomedical Circuits Systems Conf BioCAS*, pp. 33–36, 2006.

[28] C.-T. Lin, F.-C. Lin, S.-A. Chen, S.-W. Lu, T.-C. Chen, and L.-W. Ko, "EEG-based brain-computer interface for smart living environmental autoadjustment," *J Med Biol Eng*, vol. 30, pp. 237–245, 2010.

[29] G. Ruffini, S. Dunne, L. Fuentemilla, C. Grau, E. Farré, J. Marco-Pallarés, P. C. P.Watts, and S. R. P. Silva, "First human trials of a dry electrophysiology sensor using a carbon nanotube array interface," *Sens Actuators A: Phys*, vol. 144, pp. 275–279, 2008.

[30] C.-T. Lin, L.-D. Liao, Y.-H. Liu, I.-J. Wang, B.-S. Lin and J.-Y. Chang, "Novel dry polymer foam electrodes for long-term EEG measurement," *IEEE Trans Biomed Eng*, vol. 58, pp. 1200-1207, 2011.

[31] C. Crozea, C.D. Voinescu and S. Fazli, "Bristle-sensors—low-cost flexible passive dry EEG electrodes for neurofeedback and BCI applications," *J Neural Eng*, vol. 8, pp. 1-8, 2011.

[32] P. Fiedler, S. Bordkorb, C. Fonseca, F. Vaz, F. Zanow, and J. Haueisen, "Novel TiN-based dry eeg electrodes; influence of electrode shape and number on contact impedance and signal quality," in *IFMBE Proc*, Vol. 29, pp. 418–421, 2010.

[33] E. Spinelli and M. Haberman, "Insulating electrodes: a review on biopotential front ends for dielectric skin-electrode interfaces," *Physiol Meas*, vol. 31, pp. S183-98, Oct 2010.

[34] Y. M. Chi, T. P. Jung, and G. Cauwenberghs, "Dry-contact and noncontact biopotential electrodes: methodological review," *IEEE Rev Biomed Eng*, vol. 3, pp. 106-19, 2010.

[35] A. Gruetzmann, S. Hansen and J.Müller, "Novel dry electrodes for ECG monitoring," *Physiol Meas*, vol. 28, pp. 1375-1390, Nov 2008.

[36] H. J. Baek, H. J. Lee, Y. G. Lim and K. S. Park, "Conductive polymer foam surface improves the performance of a capacitive EEG electrode," *IEEE Trans Biomed Eng*, in press, 2012.

[37] H. J. Baek, H. S. Kim, J. Heo, Y. G. Lim and K. S. Park, "Brain-computer interfaces using capacitive measurement of steady-state visual or auditory responses," *J Neural Eng*, in revision, 2013.

[38] Y. M. Chi and G. Cauwenberghs, "Micropower non-contact EEG electrode with active common-mode noise suppression and input capacitance cancellation," in *Conf Proc IEEE Eng Med Biol Soc*, pp. 4218-4221, 2009.

[39] Y. M. Chi and G. Cauwenberghs, "Wireless non-contact EEG/ECG electrodes for body sensor networks," in *Proc Int Conf Body Sensor Networks (BSN)*, pp. 297-301, 2010.

[40] Y. G. Lim, K. K. Kim and K. S. Park, "ECG measurement on a chair without conductive contact," *IEEE Trans Biomed Eng*, vol. 53, pp. 956-959, 2006.

[41] Y. G. Lim, K. K. Kim and K. S. Park, "ECG recording on a bed during sleep without direct skin-contact," *IEEE Trans Biomed Eng*, vol. 54, pp. 718-725, 2007.

[42] S. M. Lee, K. S. Sim, K. K. Kim, Y. G. Lim and K. S. Park, "Thin and flexible active electrodes with shield for capacitive electrocardiogram measurement," *Med Biol Eng Comput*, vol. 48, pp. 447-457, 2010.

[43] M. Blanco-Velasco, B. Weng, and K. E. Barner, "ECG signal denoising and baseline wander correction based on the empirical mode decomposition," *Comput Biol Med*, vol. 38, pp. 1-13, Jan 2008.

[44] Y. G. Lim, G. S. Chung and K. S. Park, "Capacitive Driven-right-leg Grounding in Indirect-contact ECG Measurement," in *Proc IEEE Eng Med Biol Soc Conf*, pp.1250-1253, Aug 2010.

[45] K. K. Kim, K. K. Lim and K. S. Park, "Common Mode Noise Cancellation for Electrically Non-Contact ECG Measurement System on a Chair," in *Proc IEEE Eng Med Biol Soc Conf*, pp.5881-5883, Sep 2005.

[46] Bruce B. Winter, John G. Webster, "Driven-Right-Leg Circuit Design," *IEEE Trans Biomed Eng*, vol.30, no.1, pp.62-66, Jan 1983.

[47] H. J. Baek, H. J. Lee, H. N. Yoon, Y. G. Lim and K. S. Park, "Common-mode Interference supression for capacitive measurement of electroencephalogram," in *Proc Int Conf Ubiquitours Healthcare*, pp. 127-129, 2012.

[48] I. Volosyak, D. Valbuena, T. Malechka, J. Peuscher and A. Gräser, "Brain-computer interface using water-based electrodes," *J Neural Eng*, vol. 7, 066007, 2010.

[49] I. Volosyak, H. Cecotti, D. Valbuena and A. Gräser, "Evaluation of the Bremen SSVEP based BCI in real world conditions," in *Proc IEEE ICORR'09*. pp.322-31, 2009.

[50] B. Allison, T. Lüth, D. Valbuena, A. Teymourian, I. Volosyak and A. Gräser, "BCI demographics: how many (and what kinds of) people can use an SSVEP BCI?," *IEEE Trans Neural Syst Rehabil Eng*, vol. 18, pp. 107-16, 2010.

[51] D. W. Kim, H. J. Hwang, J. H. Lim, Y. H. Lee, K. Y. Jung and C. H. Im, "Classification of selective attention to auditory stimuli: toward vision-free brain-computer interfacing," *J Neurosci Methods*, vol. 197, pp. 180-5, 2011.

[52] M. A. Pastor, J. Artieda, J. Arbizu, J. M. Marti-Climent, I. Penuelas and J. C. Masdeu, “Activation of human cerebral and cerebellar cortex by auditory stimulation at 40Hz,” *J Neurosci*, vol. 22 pp. 10501-6, 2002.

[53] Y. M. Chi, Y. T. Wang, Y. Wang, C. Maier, T. P. Jung and G. Cauwenberghs, ”Dry and noncontact EEG sensors for mobile brain-computer interface,” *IEEE Trans Neural Syst Rehabil Eng*, vol. 20, pp. 228-35, 2012.

[54] H. J. Baek, G. S. Chung, K. K. Kim, and K. S. Park, "A smart health monitoring chair for nonintrusive measurement of biological signals," *IEEE Trans Inf Technol Biomed*, vol. 16, pp. 150-8, Jan 2012.

[55] S. M. Lee, K. K. Kim and K. S. Park, “Wavelet approach to artifact noise removal from capacitive coupled electrocardiograph,” in *Proc IEEE Eng Med Biol Soc Conf*, pp. 2944-2947, Aug 2008.

[56] J. T. Gwin, K. Gramann, S. Makeig and D. P. Ferris, “Removal of movement artifact from high-density EEG recorded during walking and running,” *J Neurophysiol*, vol. 103, pp. 3526-3534, Jun 2010.

[57] B. Eilebrecht, T. Wartzek, J. Willkomm, A. Schommartz, M. Walter, and S. Leonhardt, “Motion artifact removal from capacitive ECG measurements by means of adaptive filtering,” in *Proc 5th Eur Conf Int Feder Med Biol Eng*, pp. 902–905, 2012.

[58] M. Oehler, P. Neumann, M. Becker, G. Curio, and M. Schilling, "Extraction of SSVEP signals of a capacitive EEG helmet for human machine interface," in *Conf Proc IEEE Eng Med Biol Soc*, vol. 2008, pp. 4495-8, 2008.

[59] L. D. Liao, C. T. Lin, K. McDowell, A. E. Wickenden and K. Gramann, “Biosensor technologies for augmented brain-computer interfaces in the next decades,” *Proc IEEE*, vol. 100, pp. 1553-66, 2012.

[60] H. J. Baek, H. J. Lee, Y. G. Lim and K. S. Park, “Investigations of capacitively-coupled EEG electrode for use in brain-computer interface,” in *Conf Proc IEEE Sys, Man Cyber,* pp. 278-282, 2012.

Appendix

Capacitively Measured EEG Responses under State-of-the Art BCI Paradigms

The offline experiments were performed to detect occipital alpha rhythm, steady state visual evoked potential (SSVEP), visual evoked P300 event related potential (P300), steady-state auditory response (ASSR), and motor imaginary sensory motor rhythm (MI) [60]. Electrodes were placed according to the international 10-20 system. The EEG data were recorded with capacitively coupled electrodes at *Oz* for alpha and SSVEP detection, at *Pz* for P300 and *C3* for MI. All signals were recorded with a reference electrode at *A2*. A dummy electrode was placed at *Fpz* for grounding. Signals were measured through hair and transmitted through a hardware module composed of a high-pass filter (HPF), low-pass filter (LPF), 60Hz notch filter (NF), and an amplifier. The HPF and LPF were used to reduce fluctuation and for anti-aliasing, respectively, and designed as Butterworth filters from 0.05 to 30 Hz. EEGs were digitized at a 512Hz sampling rate using an analog-to-digital converter (NI-DAQ Pad 6015, National Instruments Co., TX, USA) and recorded using a BCI2000 general purpose software platform developed by the BCI Group at the Wadsworth Center, USA [20]. The BCI2000 data files were analyzed using a Matlab MEX file

that is included with the BCI2000 distribution package.

The subject was asked to open or close his eyes during 30s each for alpha rhythm detection. A counterphased flickering checkerboard pattern was employed for SSVEP experiments. The frequencies presented to subjects were f =(5.45, 6.667, 7.5, 8.57, 10, 12, 15,20) Hz. Stimuli were generated on a PC using Matlab with Psychtoolbox and presented on a 19" flat screen monitor (FLATRON Slim, LG Electronics Ltd., Korea). Each subject was instructed to focus his eyes on the checkerboard pattern for 60s. The P300 matrix speller described by Farwell and Donchin was employed for P300 experiments and was controlled using the BCI2000 software platform. The subject's task was to focus his attention on target characters, one by one, in the matrix and to note the number of times they flashed. The words spelled were "THE QUICK BROWN FOX" and they were presented above the matrix. Each letter flashed 15 times for each selection and the duration of each stimulus was 80ms. For ASSR experiment, auditory stimuli of two different frequencies to the left and right ear were given simultaneously. The subject's task was selective attention to left or right stimulus. I chose 37Hz and 43Hz, as the modulation frequencies. The carrier frequencies of the two auditory stimuli were set to 1kHz and 2.5kHz, respectively, so the subject could easily recognize each sound stimulus.

Finally, the subject was given a task to perform involving imaginary right hand

movements according to a cue. Experiment consisted of 120s resting state recording and 120s imagery movement recording. During imagery movement session, the subject opened and closed his right hand imaginarily with the fingers opening and closing from the palm of the hand at a rate of approximately 1 Hz. The log ratio of the power during the imagery movement condition relative to the power during the resting condition was then calculated. A log ratio of less than zero indicates suppression whereas a value greater than zero indicate enhancement and value of zero indicates no changing.

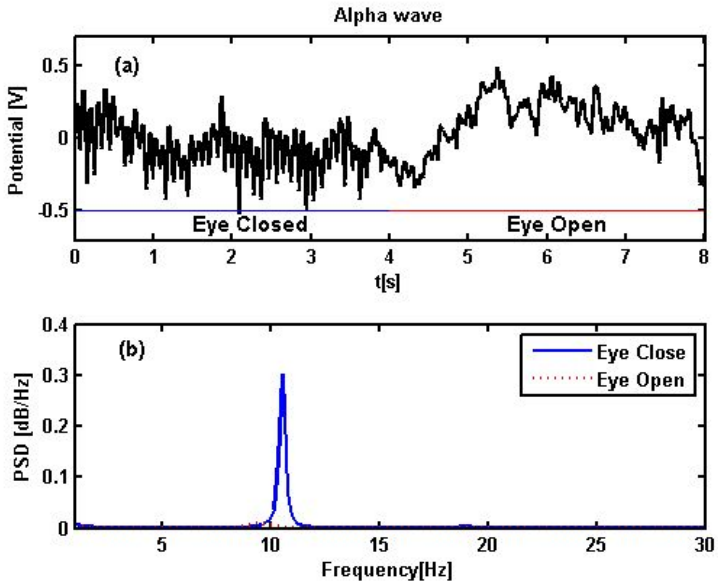

Figure A-1. The EEG alpha rhythm measured using a cap installed with capacitively-coupled electrodes. (a) time domain EEG signal and (b) its spectrum.

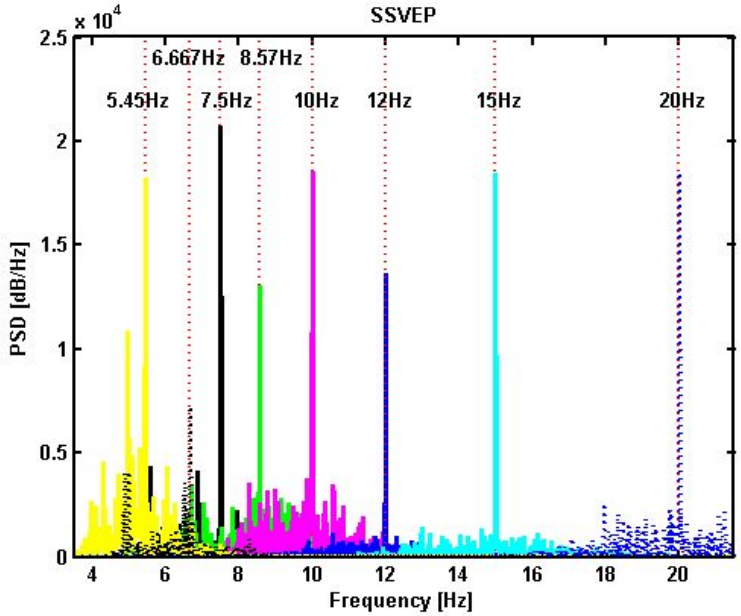

Figure A-2. SSVEP responses for 8 kinds of visual stimulus frequencies measured through dry hair by a cap with capacitively-coupled electrodes.

Alpha rhythm signals were successfully obtained from electrode attached at the Oz site through dry hair (Figure A-1). As expected, the alpha frequency range from 8Hz to 14Hz dominated the spectrum during closed-eye sessions. Figure A-2 shows SSVEP responses to checkerboard visual stimulation. Capacitively measured EEG clearly responded to visual stimulation as shown by the distinct peaks at the stimulus frequencies. Similar to the results of our previous frequency response experiments, the spectral power of relative background noise was higher at relatively low stimulus frequencies.

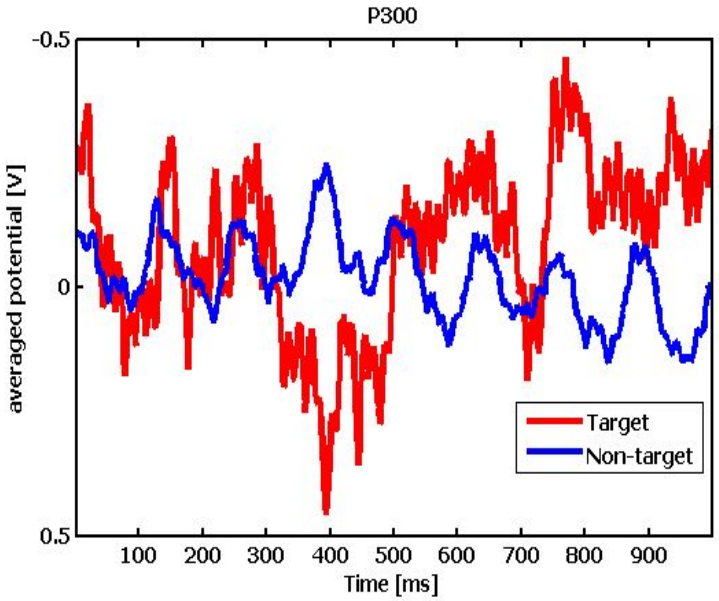

Figure A-3. Capacitively measured P300 signal through dry hair using a cap with capacitively-coupled electrodes.

Figure A-3 shows the average responses for P300 experiments. Compared to responses during non-target presentations (dashed line), positive deflection was detected during the period from 300-600ms when subjects detected an occasional target stimulus among the standard matrix stimuli (solid line). The value of the coefficient of determination (r-squared) for target and non-target distributions was highest (>0.005) in the 300-600ms range (<0.00005). This difference between desired and undesired brain responses was statistically significant.

The spectral power around the frequency of sensorimotor rhythm (8-13Hz) for a

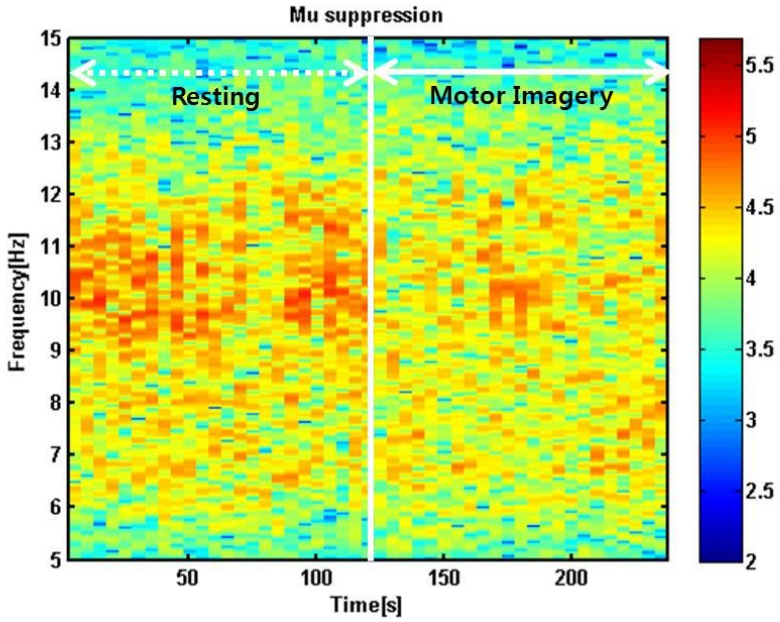

Figure A-4. The EEG mu rhythm suppression recorded by capacitively-coupled electrode during imagery movement started from 120ms after starting of measurement.

location over the left sensorimotor cortex is shown in figure A-4. The powers of those frequency ranges were suppressed during motor imagery by forming the log ratio value less than zero (-0.3141).

Figure A-5 shows the power spectral density at C_z electrode averaged across trials with respect to two different conditions under ASSR experiment: attention to left ear's stimulus sound versus attention to right ear's stimulus sound. The spectrum presented in figure A-5 shows two distinct stimulus frequencies peaking at 37Hz and

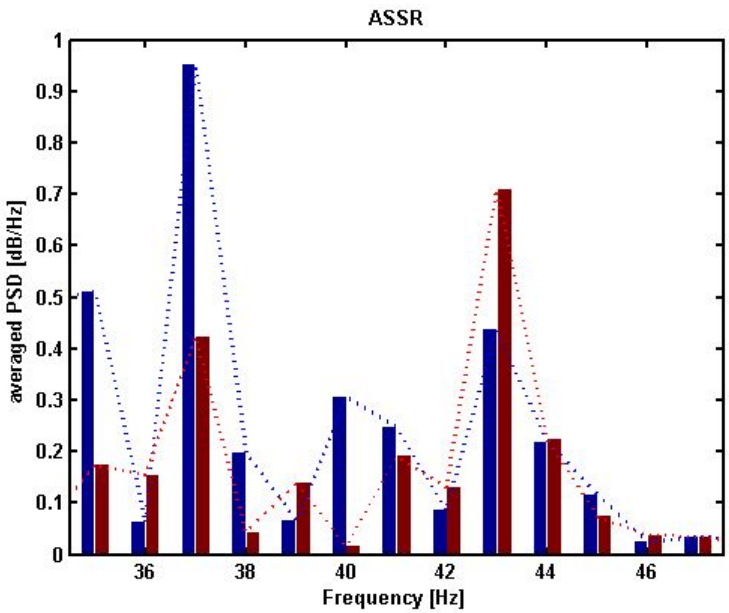

Figure A-5. The EEG spectral density plot averaged across the trials with respect to two different conditions (red: attending to the left auditory stimulus condition (37Hz amplitude modulation), blue: attending to the right stimulus condition (43Hz amplitude modulation)).

43Hz and the EEG power spectral density was also modulated by selective attention to stimulus sound source. In figure A-5, the blue bar indicates spectral power when the subject attended to the left stimulus sound of 37Hz and red bar indicates those when the subject attended to the right stimulus sound of 43Hz.

국문 초록

뇌-컴퓨터 인터페이스 기술은 신경 근육 활동과 완전히 독립적인 대안적 의사소통 도구로서 광 범위하게 연구되고 있다. 현재, 뇌파 기반의 시스템이 가장 널리 사용되는데, 이는 불쾌감을 주는 겔 주입, 비실용적인 준비과정 및 사용 후 세척과정을 요구한다. 때문에 차세대 뇌-컴퓨터 인터페이스 기술은 연구 결과의 실제 환경 적용을 위해 실용적이고 사용자 친화적인 무구속 뇌파 측정 플랫폼을 요구한다. 용량성 결합의 전극은 전해질 겔 및 직접적인 두피 접촉을 필요로 하지 않아 현재의 습식 전극 시스템을 대체할 수 있는 미래 기술로서의 잠재력을 지니고 있다.

본 논문에서는 임상 외 환경에서 무구속적으로 뇌파를 측정할 수 있는 용량성 결합의 전극으로 사용하기 위하여 전도성 폴리머 폼 표면의 전극이 제안되었다. 기존의 용량성 결합의 전극은 신호 감지를 위한 전극 표면이 딱딱하여 그 강성에 의해 머리의 굴곡면이나 머리카락으로 인해 발생되는 분리된 공간에 안정적인 접촉 면적을 제공할 수 없어 용량성 결합을 이용한 뇌파 측정을 어렵게 만든다. 이 문제를 해결하기 위하여 완충효과를 제공하는 폴리머 폼을 고입력 임피던스의 능동 전극 표면에 적용하였으며, 이를 통하여 두피와의 전기적 접촉 없이 머리카락을 통하여

뇌파를 측정할 수 있었다. 실험 결과, 제안된 전극은 기존의 전극과 비교하여 더 낮은 전극-피부 간 임피던스, 더 높은 전압 이득, 신호 대 잡음 비, 신호 대 오차 비를 보여주었으며, 용량성 결합의 전극과 기존의 전도성 습식 전극으로 동시에 측정한 뇌파 신호들 간의 상관관계분석에서 제안된 용량성 결합의 전극이 종래의 용량성 결합의 전극보다 더 높은 상관계수를 보여주었다. 또한 기존의 용량성 결합의 전극에서는 측정하지 못한 뇌파 신호를 제안된 전극으로는 측정 가능했던 경우도 존재했다.

제안된 폼 표면의 용량성 결합의 뇌파 전극을 5명의 피실험자에 대하여 안정상태 시각 유발 전위 혹은 청성 안정 유발 반응 기반 패러다임의 뇌-컴퓨터 인터페이스 실험을 진행하였다. 이를 위하여 안정 상태 시각 유발 전위 기반의 가상 키보드 시스템과 청성 안정 유발 반응 기반의 이진 분류 시스템이 사용되었다. 실험 결과, 오프라인 분석에서 두 종류의 실험에서 뇌-컴퓨터 인터페이스 기술에 적용 가능할 정도의 성능을 보여주었다. (안정 상태 시각 유발 전위 기반 시스템의 정확도: 95.2%, 청성 안정 유발 반응 기반 시스템의 정확도: 82.6%). 온라인 실험에서는 안정 상태 시각 유발 전위 기반의 가상 키보드 시스템에서 주어진 단어를 입력하도록 하고 안정 상태 청성 반응 기반의 이진 분류 시스템에서는 선택적으로 자극에 집중하도록 하였는데, 평균 정보전달율이 각각 분당 17.28±2.08 비트, 0.7±0.24비트로 측정되었다.

본 논문의 실험 결과는 뇌-컴퓨터 인터페이스 시스템을 포함하는 뇌파 측정 시스템에서 제안된 폼 표면의 용량성 결합의 전극을 사용할 수 있는 가능성을 보여주었다. 제안된 전극은 차세대 뇌-컴퓨터 인터페이스 기술의 다양한 응용을 위한 유연하고 무구속적인 도구가 될 수 있다. 제안된 전극은 모자나 헬멧에 설치되어 사용자의 외관을 이상하게 보이지 않도록 하는 착용형 시스템으로 쉽게 응용될 수 있으며, 실제 뇌파를 기반으로 한 여러 응용 기술에서 사용 가능하리라 기대한다.

핵심어: 생체 신호 측정 전극, 뇌-컴퓨터 인터페이스, 용량성 결합의 전극, 뇌전도, 폴리머 폼.

학 번: 2009-3026